308 --- Q19960322001G
Scientific Notebook #14B for
Subregional Hydrogeology
Research Project

9/5/96
RT

Scientific Notebook for "Subregional Hydrogeology"
Research Project.

20-5704-175

Contents

Page

Entries by:
David R. Turner - DRJ
JOYCE L. FOECELLE - JF
Timothy L. Tolley TLT
Ross Baftzoglou RB

First 150 pages are devoted to entries by the following people: David Turner, Joyce Foegelle, & Tim Tolley.

The other 150 pages are devoted to entries of: Tim Tolley & Ross Baftzoglou.

5/9/95 - DRJ

Subregional Hydrolgeologic Flow and Transport Research Project:

Task 5 - Characterization of the Potential for Present or Future Perched-Water Development

The purpose of this task is to identify and study, if possible, areas where perched-water zones may have formed in the geologic past, or might form in the future under different hydrologic and climatological conditions. Most of the focus of this task will be on the Yucca Mountain subregion, but other areas (e.g., Apache Leap Tuff Site, Pena Blanca Analog site) may be considered due to specific data needs. This task is currently designed to provide information to the flow and transport modeling task, largely in the form of geologic and geochemical information that can be used to constrain model boundary and initial conditions as well as confirm model results.

The effort will focus on evaluating and compiling geochemical data available in the Yucca Mountain subregion. These data will largely be composed of geochemical site characterization data obtained by DOE and its contractors, although there may be some data from other sources (e.g., Nevada Bureau of Mines and Geology reports, peer-reviewed literature, etc). These data will be registered within 2D geographic information systems (ARC/INFO) and 3D geologic framework models (EarthVision) currently in development at CNWRA.

Data sources will be documented and referenced as the data are entered into the database. CNWRA-generated laboratory and field data will meet quality assurance (QA) requirements described in the CNWRA QA Manual. In addition, data obtained from DOE site characterization activities will likely meet DOE QA requirements. Data from other sources, however, will be freely used as necessary. For data from these sources, the referenced sources should be consulted for determining their level of QA.

6-2-95 JF

SOURCES USED FOR DATA

Benson, L.V., and McKinley, P.W. 1985. Chemical Composition of Ground Water in the Yucca Mountain Area, Nevada, 1971-1984. USGS Open-File Report 85-484.

Bish, D.L., and Chipera, S.J. 1989. Revised Mineralogic Summary of Yucca Mountain, Nevada. Los Alamos National Laboratory LA-11497-MS.

Carlos, B.A. 1987. Minerals in Fractures of the Saturated Zone from Drill Core USW G-4, Yucca Mountain, Nye County, Nevada. Los Alamos National Laboratory LA-10927-MS.

Chipera, S.J., and Bish, D.L. 1989a. Quantitative X-Ray Diffraction Analyses of Samples used for Sorption Studies by the Isotope and Nuclear Chemistry Division, Los Alamos National Laboratory. Los Alamos National Laboratory LA-11669-MS.

Chipera, S.J., and Bish, D.L. 1989b. The Occurrence and Distribution of Erionite at Yucca Mountain, Nevada. Los Alamos National Laboratory LA-11663-MS.

Fabryka-Martin, J.T., Wightman, S.J., Murphy, W.J., Wickham, M.P., Caffee, M.W., Nimz, G.J., Southon, J.R., Sharma, P. 1993. Distribution of Chlorine-36 in the unsaturated zone at Yucca Mountain: An indicator of fast transport paths. Conference Proceedings FOCUS '93: Site Characterization and Model Validation: 58-68.

Mower, T.E., Higgins, J.D., Yang, I.C., and Peters, C.A. 1994. Pore-Water Extraction from Unsaturated Tuff by Triaxial and One-Dimensional Compression Methods, Nevada Test Site, Nevada. USGS Water-Resources Investigations Report 93-4144.

Szabo, B.J., and Kyser, T.K. 1990. Ages and stable-isotope composition of secondary calcite & opal in drill cores from Tertiary rocks of the Yucca Mountain area, Nevada. Geological Society of America Bulletin 102(12): 1714-1719.

Whelan, J.F., and Stuckless, J.S. 1992. Paleohydrologic implications of the stable isotopic composition of secondary calcite within the Tertiary volcanic rocks of Yucca Mountain, Nevada. High-Level Radioactive Waste Management. Proceedings of the Third International Conference: 1572-1581.

6-2-95 JF

SOURCES USED FOR DATA (continued)

Whelan, J.F., Vaniman, D.T., Stuckless, J.S., and Moscati, R.J. 1994. Paleoclimatic and paleohydrologic records from secondary calcite: Yucca Mountain, Nevada. High-Level Radioactive Waste Management. Proceedings of the Fifth International Conference: 2738-2745.

JF Yang, I.C. 1992. Flow and transport through unsaturated rock. Data from two test holes, Yucca Mountain, Nevada. High-Level Radioactive Waste Management. Proceedings of the Third International Conference: 732-737.

Yang, I.C., Turner, A.K., Sayre, T.M., and Montazer, P. 1988. Triaxial-Compression Extraction of Pore Water from Unsaturated Tuff, Yucca Mountain, Nevada. USGS Water-Resources Investigations Report 88-4189.

6-2-95 JF

TABLULAR DATA FROM THESE SOURCES IS IN FILE QPRO/MINWT.WQ1 ON A DISKETTE IN THE BACK POCKET.

Bish, D.L., and Chipera, S.J. 1989. Revised Mineralogic Summary of Yucca Mountain, Nevada. Los Alamos National Laboratory LA-11497-MS.
Appendix A, pages 18 through 49 entered into QPRO\MINWT.WQ1 database.
Minerals assayed for: smectite, mica, clinoptilolite, mordenite, analcime, tridymite, quartz, cristobalite, opal-CT, alkali feldspar, calcite, glass, hematite, and the rare occurrences of hornblende, chlorite, calcite, kaolinite, fluorite, todorokite, laumontite, illite, mordenite, and cryptomelane.
Wells studied: J-12, J-13, UE-25a#1, UE-25b#1H, UE-25p#1, USW G-1, USW G-2, USW GU-3, USW G-4, USW H-3, USW H-4, USW H-5, USW H-6, USW WT-1, and USW WT-2.

JF

Chipera, S.J., and Bish, D.L. 1989a. Quantitative X-Ray Diffraction Analyses of Samples used for Sorption Studies by the Isotope and Nuclear Chemistry Division, Los Alamos National Laboratory. Los Alamos National Laboratory LA-11669-MS.
Appendix I, pages 12 through 18 entered into QPRO\MINWT.WQ1 database.
Minerals assayed for: smectite, mica, clinoptilolite, mordenite, analcime, quartz, cristobalite, opal-CT, alkali feldspar, glass, hematite, and rare occurrences of calcite, tridymite, kaolinite, and hornblende.
Wells studied: J-13, UE-25a#1, USW G-1, USW G-2, USW GU-3/G-3, and USW G-4.

Chipera, S.J., and Bish, D.L. 1989b. The Occurrence and Distribution of Erionite at Yucca Mountain, Nevada. Los Alamos National Laboratory LA-11663-MS.
Table I, pages 6 through 8 is composed almost entirely of the mineral abundances from Bish and Chipera, 1989, Revised Mineralogic Summary of Yucca Mountain, LANL 11497. Two exceptions are for the fracture samples J13-1345 and UE-25a#1-1296.2. Also, there are two erionite values for J12-620/630 and USW G4-1314 which are not noted in the Bish and Chipera, 1989 report. These four are the only data entered into QPRO\MINWT.WQ1.

6295 JF

TABLULAR DATA FROM THESE SOURCES FOLLOWS.

Benson, L.V., and McKinley, P.W. 1985. Chemical Composition of Ground Water in the Yucca Mountain Area, Nevada, 1971-1984. USGS Open-File Report 85-484.
Table 1, page 4 entered into QPRO\ISOTOPE.WQ1.
Assays for: δD, $\delta^{18}O$, $\delta^{13}C$, ^{14}C, ^{14}C apparent age, and HTO.
Wells studied: J-12, J13, UE-25b#1, UE-25c#1, UE-25c#2, UE-25c#3, UE-25p#1, UE-29a#2, USW G-4, USW H-1, USW H-3, USW H-4, USW H-5, USW H-6, USW VH-1.

Carlos, B.A. 1987. Minerals in Fractures of the Saturated Zone from Drill Core USW G-4, Yucca Mountain, Nye County, Nevada. Los Alamos National Laboratory LA-10927-MS.
Table I, page 7 entered into QPRO\MINWT.WQ1 database.
Minerals assayed for: smectite, clinoptilolite, mordenite, quartz, cristobalite, alkali feldspar, calcite, and mica.
Well studied: USW G-4.

JF

Fabryka-Martin, J.T., Wightman, S.J., Murphy, W.J., Wickham, M.P., Caffee, M.W., Nimz, G.J., Southon, J.R., Sharma, P. 1993. Distribution of Chlorine-36 in the unsaturated zone at Yucca Mountain: An indicator of fast transport paths. Conference Proceedings FOCUS '93: Site Characterization and Model Validation: 58-68.
Table 2 entered into QPRO\ISOTOPE.WQ1.
Assays of: Cl/Br and $^{36}Cl/Cl \times 10^{-15}$.
Borehole cuttings from: USW UZ-N11, USW UZ-N37, USW UZ-N53, USW UZ-N53, USW UZ-N55, UE-25 UZ16.

Mower, T.E., Higgins, J.D., Yang, I.C., and Peters, C.A. 1994. Pore-Water Extraction from Unsaturated Tuff by Triaxial and One-Dimensional Compression Methods, Nevada Test Site, Nevada. USGS Water-Resources Investigations Report 93-4144.
Table 10, page 46.
Minerals assayed for: sanidine, albite, quartz, cristobalite, amorphous silica, clinoptilolite, ferric illite, illite/montmorillonite, chlorite, pyrite, rutile, goethite, calcite, and biotite.
One well studied: UE-25 UZ#5. Two samples noted as UZ5-335 and UZ5-347.

6

6-2-95 JF

JF

FROM:

Benson, L.V., and McKinley, P.W. 1985. Chemical Composition of Ground Water in the Yucca Mountain Area, Nevada, 1971-1984. USGS OFR 85-484. Table 1, p.4.

Table 1.--*Chemical composition of water samples obtained from test wells*

[m, meters; δD, del deuterium, reported in parts per thousand, o/oo, relative to SMOW (standard mean ocean water); $\delta^{18}O$, del oxygen-18, reported in parts per thousand, o/oo, relative to SMOW; $\delta^{13}C$, del carbon-13, reported in parts per thousand, o/oo, relative to PDB (Peedee belemnite); ^{14}C, carbon-14; yr B.P., years before present; HTO, tritium, reported in picocuries per liter; °C, degrees Celsius; dissolved constituents: Ca (calcium), Mg (magnesium), Na (sodium), K (potassium), HCO_3 (bicarbonate), Cl (chloride), SO_4 (sulfate), SiO_2 (aqueous silica), F (fluoride), O_2 (dissolved oxygen), and dissolved solids reported in milligrams per liter, except Li (lithium) and Sr (strontium), which are reported in micrograms per liter; ---, indicates entire well bore pumped; --, indicates that no data are available for particular analysis of interest; *, certain dissolved oxygen (O_2) values taken from Ogard and Kerrisk (1984)]

Test well designation	Land-surface altitude (m)	Approximate well depth (m)	Approximate depth to water (m)	Interval sampled (m)	Collection date	δD o/oo SMOW	$\delta^{18}O$ o/oo SMOW	$\delta^{13}C$ o/oo PDB	^{14}C percent modern	^{14}C Apparent age (yr B.P.)	HTO	*O_2	Specific conductance (microsiemens per centimeter at 25° C) Onsite	Specific conductance (microsiemens per centimeter at 25° C) Laboratory
J-12	953.5	347	225	---	03/26/71	-97.5	-12.8	-7.9	32.2	9,100	<220	--	285	252
J-13	1,011.3	1,063	282	---	03/26/71	-97.5	-13.0	-7.3	29.2	9,900	<220	5.7	285	252
UE-25b#1	1,200.4	1,220	470	---	08/07/81	-99.5	-13.4	-10.7	--	--	--	1.8	318	319
UE-25b#1	1,200.4	1,220	470	---	09/01/81	-101	-13.4	-10.4	16.7	14,400	<200	--	300	281
UE-25b#1	1,200.4	1,220	470	(863-875)	07/20/82	-99.5	-13.5	-8.6	18.9	13,400	2	1.6	291	297
UE-25c#1	1,131.0	914	400	---	09/30/83	-102	-13.5	-7.1	15.0	15,200	<1	--	290	310
UE-25c#2	1,132.0	913	401	---	03/13/84	-100	-13.4	-7.0	16.6	14,400	<2	--	295	303
UE-25c#3	1,132.0	913	402	---	05/09/84	-103	-13.5	-7.5	15.7	14,900	2	--	298	309
UE-25p#1	1,114.0	1,800	381	(381-1,197)	02/09/83	-106	-13.5	-4.2	3.5	26,900	<10	--	628	639
UE-25p#1	1,114.0	1,800	361	(1,297-1,805)	05/12/83	-106	-13.8	-2.3	2.3	30,300	10	1.3	1,120	1,120
UE-29a#2	1,215.1	422	29	(247-354)	01/08/82	-93.5	-12.8	-13.0	62.3	3,800	37	5.4	240	255
UE-29a#2	1,215.1	422	29	(87-213)	01/15/82	-93.0	-12.8	-13.1	60.0	4,100	37	5.6	258	317
USW G-4	1,270.0	915	541	---	12/09/82	-103	-13.8	-9.1	22.0	12,160	--	6.4	312	307
USW H-1	1,302.2	1,829	572	(572-687)	10/20/80	-103	-13.4	--	19.9	13,000	<20	--	255	258
USW H-1	1,302.2	1,829	572	(687-1,829)	12/08/80	-101	-13.5	-11.4	23.9	12,000	<20	--	247	266
USW H-3	1,483.0	1,220	--	(822-1,220)	03/14/84	-101	-13.9	-4.9	10.5	18,100	2	<0.1	523	535
USW H-4	1,249.0	1,220	519	---	05/17/82	-104	-14.0	-7.4	11.8	17,200	<10	5.8	340	381
USW H-5	1,477.8	1,220	704	---	07/03/82	-102	-13.6	-10.3	18.2	13,700	<200	6.3	275	273
USW H-5	1,477.8	1,220	704	---	07/26/82	-102	-13.6	-10.3	21.4	12,400	<200	--	278	276
USW H-6	1,302.0	1,220	526	---	10/16/82	-106	-13.8	-7.5	16.3	14,600	<10	5.9	372	--
USW H-6	1,302.0	1,220	--	(753-835)	06/20/84	-105	-14.0	-7.3	10.0	18,500	4	--	360	392
USW H-6	1,302.0	1,220	--	(608-646)	07/06/84	-107	-14.0	-7.1	12.4	16,800	1	--	402	408
USW VH-1	954.5	762	184	---	02/06/81	--	--	--	--	--	--	--	370	410
USW VH-1	954.5	762	184	---	02/08/81	--	--	--	--	--	--	--	395	397
USW VH-1	954.5	762	184	---	02/11/81	-108	-14.2	-8.5	12.2	17,000	<20	--	388	402

FROM:

Carlos, B.A. 1987. Minerals in fractures of the Saturated Zone from Drill Core USW G-4, Yucca Mountain, Nye County, Nevada. LANL 10927-MS. Table I on page 7.

TABLE I

SEMIQUANTITATIVE X-RAY DIFFRACTION ANALYSES OF FRACTURE FILLINGS IN USW G-4, SATURATED ZONE

Sample (ft) Depth	Est. Fract Coverage %	Est. Max % Contamination	Smectite	Clinoptilolite	Mordenite	Quartz	Cristobalite	AF	Other
1788	95	2	--	--	100	--	--	--	--
1970	Not readily discernible from rock matrix		--	10	80	10	--	--	--
1991 orange	70	20	tr	10	30	10	tr	50	--
1991 black*	Not determined, intergrown with rock grains		10	30	50	10	--	--	--
2062	60	10	--	20	75	5	--	--	--
2071	80	30	--	20	60	20	--	--	--
2099*	95	3	--	95	tr	tr	5	--	--
2100 horiz*	85	10	--	90	--	10	--	--	--
2100 white	80	5	--	5	95	tr	--	--	--
2101 white	95	1	--	10	90	tr	--	--	--
2101 beige	95	1	--	10	75	5	--	10	--
2135	100	5	--	--	--	--	100	--	--
2147 white	90	15	--	50	50	tr	--	--	--
2147 pink	95	10	--	15	75	5	--	5	--
2248	90	15	--	40	40	tr	--	20	--
2344	95	20	--	--	--	70	tr	30	--
2578*	100	20	--	--	--	60	tr	10	30[a]
2615*	95	7	--	--	--	30	--	70	--
2689	Not readily discernible from rock matrix		40	--	--	40	--	20	--
2698	100	5	--	60	30	--	10	--	--
2728	90	10	--	tr	100	tr	--	--	--
2793	100	2	--	90	10	--	--	--	--
2823	100	1	5	5	80	10	--	--	--
2832	98	5	20	20	50	10	--	--	--
2854*	Not determined, intergrown with rock matrix		--	--	--	40	--	60	tr[b]
2931	30	10	40	--	20	40	--	--	--
2947	100	5	--	--	--	100	--	--	--
2955*	85	15	--	--	--	40	--	60	--
2967*	90	5	--	--	--	60	--	40	--
2985	90	10	--	--	--	100	--	tr	--

* Sample contains manganese oxides. Percentages are relative for other minerals in sample, and no estimate of actual abundances has been attempted.

[a] Calcite.

[b] Mica.

Fabryka-Martin, etal. 1993. Distribution of Chlorine-36 in the unsaturated zone at Yucca Mountain: An indicator of fast transport paths. Conference Proceedings FOCUS '93: Site Characterization and Model Validation; 26-29 September 1993, Las Vegas, NV. p.61.

Table 2. Halide and ^{36}Cl analyses of borehole cuttings

Table 2.

Sample ID	Top of interval (ft)	mg Cl /kg rock	Cl/Br Ratio	Measured $^{36}Cl/Cl$ x 10^{-15}	Ther./ Mech. Unit
USW UZ-N11					
R149	15	n.m.	n.m.	1000 ± 50	TCw
R152	31	6	113	696 ± 23	PTn
R154	41	7	129	923 ± 13	PTn
R157	55	3	964	1082 ± 37	PTn
R159	65	3	281	13060 ± 250	PTn
R162	80	4	216	10100 ± 700	PTn
USW UZ-N37					
R95	5	3	36	1350 ± 38	UO
R98	11	58	205	1230 ± 17	UO
R101	20	4	213	1158 ± 24	UO
R103	24	n.m.	n.m.	1112 ± 29	UO
R107	30	5	110	35 ± 64	UO
R112	36	5	260	161 ± 6	TCw
R285	110	n.m.	n.m.	504 ± 22	PTn
R288	125	4	78	253 ± 10	PTn
R293	148	4	423	327 ± 6	PTn
R298	174	6	226	847 ± 12	PTn
R301	189	5	n.m.	575 ± 124	PTn
R307	217	4	41	850 ± 105	PTn
R312	242	7	844	269 ± 6	PTn
Note: PTn/TSw1 contact @ 256.7 ft					
USW UZ-N53					
R349	124	6	376	2006 ± 69	TCw
R351	134	n.m.	n.m.	2050 ± 90	TCw
R353	144	3	248	4561 ± 130	PTn
R361	183	6	126	2369 ± 34	PTn
R364	198	3	168	710 ± 36	PTn
R366	208	10	301	522 ± 17	PTn
Note: PTn/TSw1 contact @ 230.7 ft					
USW UZ-N54					
R002	5	9	80	3719 ± 175	UO
R003	7	62	180	1098 ± 33	UO
R004	10	84	166	687 ± 35	UO
R005	12	152	208	556 ± 21	UO
R006	15	206	195	526 ± 22	UO
R007	17	148	230	501 ± 21	UO
R008	22	102	247	507 ± 14	UO
R033	135	10	300	277 ± 19	PTn
R034	140	9	267	149 ± 22	PTn
R117	165	8	60	402 ± 9	PTn
R121	184	7	222	480 ± 16	PTn
R125	204	9	81	474 ± 49	PTn
R128	218	2	93	352 ± 13	PTn
R130	228	2	124	332 ± 16	PTn
Note: PTn/TSw1 contact @ 230.5 ft					
USW UZ-N55					
R035	0	2	192	1747 ± 25	UO
R040	9	3	225	5565 ± 220	TCw
R072	165	4	136	14740 ± 640	PTn
R073	170	4	143	11010 ± 190	PTn
R074	174	4	180	27040 ± 330	PTn
USW UZ-N55 (continued)					
R075	180	2	131	13157 ± 184	PTn
R078	189	8	300	1413 ± 57	PTn
R081	203	4	126	22300 ± 345	PTn
R084	218	8	161	17168 ± 1202	PTn
R087	232	5	196	6580 ± 364	PTn
R088	237	6	109	8203 ± 140	PTn
R089	242	3	109	9187 ± 220	PTn
R090	247	2	194	10480 ± 180	TSw1
R091	252	2	229	17050 ± 230	TSw1
Note: PTn/TSw1 contact @ 245.4 ft					
UE25 UZ-16					
R163	0	8	147	2280 ± 150	Fill
R165	7	58	170	615 ± 32	UO
R167	12	123	193	526 ± 16	UO
R168	14	172	198	500 ± 15	UO
R169	16	158	192	528 ± 24	UO
R170	17	104	191	750 ± 35	UO
R173	22	56	197	601 ± 26	UO
R174	24	25	179	507 ± 26	UO
R177	30	25	207	572 ± 22	UO
R178	39	7	187	1030 ± 60	UO/TCw
R182	143	1	194	106 ± 40	PTn
R183	153	1	96	346 ± 27	PTn
R184	158	1	67	329 ± 24	PTn
R185	163	1	67	338 ± 20	PTn
R186	181	2	93	306 ± 21	PTn
R187	219	2	97	434 ± 26	PTn
R205	669	1	195	145 ± 15	TSw2
R219	1090	2	213	123 ± 7	TSw2
R220	1110	3	315	117 ± 8	TSw2
R221	1122	1	157	150 ± 9	TSw3
R224	1166	1	n.m.	272 ± 16	CHn1
R225	1170	1	142	363 ± 34	CHn1

n.m. - not measured

Notes:

1. Thermal/mechanical units:[5,15] UO - Undifferentiated overburden; TCw - Moderately to densely welded Tiva Canyon; PTn - Non to moderately welded and bedded zones of Tiva Canyon, Yucca Mountain, Pah Canyon and Topopah Spring members; TSw1 - Moderately to densely welded Topopah Spring member; TSw2 - Densely welded Topopah Spring, potential repository horizon; TSw3 - Lower vitrophyric zone, Topopah Spring; CHn1 - Partially welded to nonwelded and bedded zones of Topopah Spring member, tuffaceous beds of Calico Hills Formation
2. Preliminary estimates of unit contacts provided by D.C. Buesch.[14]
3. In some cases, Cl and Br concentrations were measured on different sample aliquots than those used to obtain ^{36}Cl analyses. Where more than one ^{36}Cl analysis is available for a given sample, a weighted average ratio is reported.
4. These data are preliminary and have not yet been thoroughly reviewed.

Mower, T.E., etal. 1994. Pore-Water Extraction from Unsatruated Tuff by Triaxial and One-Dimensional Compression Methods, Nevada Test Site, Nevada. USGS Water-Resources Investigations Report 93-4144. Denver, CO: USGS. Table 10. p.46.

Table 10. Mineralogical composition of tuffs by weight[1]

[Mineral content in percent by weight; --, not found]

Sample name	Sanidine	Albite	Quartz	Cristobalite	Amorphous silica	Clinoptilolite	Ferric illite	Illite/montmorillonite	Chlorite	Pyrite	Rutile	Goethite	Calcite	Biotite	Total
Nonwelded tuff, Topopah Spring Member															
UZ5-335	2.01	2.38	3.15	--	9.66	52.78	6.60	21.14	1.80	0	0.43	--	--	--	99.95
UZ5-347	6.26	--	0.42	10.94	--	76.07	2.56	--	0.19	0	--	--	--	3.42	99.86
Nonwelded tuff, Tunnel bed 5															
GTO-JJ-DB-1A-2-1	9.63	--	3.46	--	--	75.75	10.56	--	0.11	0	0.19	0.10	--	--	99.80
GT-EX-DH3-2	14.44	--	0.57	--	11.09	61.00	11.92	--	0.57	0.01	0.22	0.09	--	--	99.91
GT-EX-DH3-3	13.61	--	0.52	--	13.92	58.75	12.19	--	0.65	0.01	0.22	0.08	--	--	99.95
Densely welded tuff, Grouse Canyon Member															
GT-LD-AC2-55	51.75	13.34	22.86	--	--	--	10.56	0.55	0.17	0	0.33	--	0.20	--	99.76
GT-LD-AC2-62	43.84	14.23	31.49	--	--	1.04	9.13	--	--	0	0.23	--	--	--	99.97

[1]Mineralogical analysis by Crystal Research Laboratories, Lander, Wyoming using X-ray diffraction, X-ray fluoresence, optical petrography, and Quantitative Mineral Analysis System (QMAS) analysis program (Slaughter, 1990).

6-295 OF

TABLULAR DATA FROM THESE SOURCES FOLLOWS (continued):

Szabo, B.J., and Kyser, T.K. 1990. Ages and stable-isotope composition of secondary calcite & opal in drill cores from Tertiary rocks of the Yucca Mountain area, Nevada. Geological Society of America Bulletin 102(12): 1714-1719.

Table 1, page 1716 entered into QPRO\ISOTOPE.WQ1.
Isotopes analyzed: $^{234}U/^{238}U$, $^{230}Th/^{234}Th$, $\delta^{13}C$, and $\delta^{18}O$.
Wells studied: UE-25a#1, USW G-2, and USW G-3/GU-3.

Whelan, J.F., and Stuckless, J.S. 1992. Paleohydrologic implications of the stable isotopic composition of secondary calcite within the Tertiary volcanic rocks of Yucca Mountain, Nevada. High-Level Radioactive Waste Management. Proceedings of the Third International Conference: 1572-1581.

Table 1, page 1575 entered into QPRO\ISOTOPE.WQ1.
Assay of $\delta^{13}C$ and $\delta^{18}O$. All data used, except the duplicates from Szabo and Kyser, 1990.
Wells studied: USW G-1, USW G-2, USW G-3/GU-3, UE-25b#1, USW G-4, and UE-25p#1.

OF

Whelan, J.F., Vaniman, D.T., Stuckless, J.S., and Moscati, R.J. 1994. Paleoclimatic and paleohydrologic records from secondary calcite: Yucca Mountain, Nevada. High-Level Radioactive Waste Management. Proceedings of the Fifth International Conference: 2738-2745.

Table 1, page 2741 entered into QPRO\ISOTOPE.WQ1 database.
$\delta^{18}O$ values (SMOW).
Wells studied: USW G-2, USW G-4, UE-25a#1, and UE-25a#5.

Yang, I.C. 1992. Flow and transport through unsaturated rock. Data from two test holes, Yucca Mountain, Nevada. High-Level Radioactive Waste Management. Proceedings of the Third International Conference: 732-737.

Table 1, page 735 entered into QPRO\ISOUEUZ4.WQ1 AND QPRO\ISOUEUZ5.WQ1.
Tritium concentration in tritium units (TU).
Wells studied: UE-25 UZ#4 and UE-25 UZ#5.

Yang, I.C., Turner, A.K., Sayre, T.M., and Montazer, P. 1988. Triaxial-Compression Extraction of Pore Water from Unsaturated Tuff, Yucca Mountain, Nevada. USGS Water-Resources Investigations Report 88-4189.

Table 3, pages 33-34 entered into QPRO\EXTRACT.WQ1 database.
Ions assayed: Ca, Mg, Na, K, Si, Cl, SO_4, Fe, Mn, Sr, and Zn.
Wells studied: UE-25 UZ#4 and UE-25 UZ#5.

FROM: Szabo, B.J., and Kyser, T.K. 1990. Ages and stable-isotope compositions of secondary calcite and opal in drill cores from Tertiary volcanic rocks of the Yucca Mountain area, Nevada. Geological Society of America Bulletin 102(12): 1714-1719. Table 1, p. 1716.

TABLE 1. ANALYTICAL DATA OF FRACTURE-FILLING CALCITE, OPAL, AND ACID-INSOLUBLE WALL-ROCK MATERIAL FROM DRILL HOLES UE-25a#1, USW G-2, AND USW G-3/GU-3 IN THE YUCCA MOUNTAIN AREA

Sample depth (m)	Fraction	Uranium (ppm)	Activity ratios			Calculated age*	$\delta^{13}C$	$\delta^{18}O$
			$^{234}U/^{238}U$	$^{230}Th/^{232}Th$	$^{230}Th/^{234}U$	($\times 10^3$ yr)	(‰)	
Drill Hole UE-25a#1								
34	Calcite	0.767** ±0.015	1.17 ±0.02	2.37 ±0.07	1.02 ±0.04	310^{+80}_{-50}††	−4.52	+20.00
87	Fault gouge	5.18** ±0.10	1.09 ±0.02	0.989 ±0.030	1.06 ±0.04	n.a.	..	..
283	Calcite	5.03** ±0.10	1.47 ±0.02	22.2 ±0.7	1.04 ±0.04	310^{+70}_{-45}§§	−6.33	+17.60
611†	Calcite	3.43** ±0.07	1.29 ±0.02	72 ±3	1.19 ±0.05	>400	−5.41	+15.60
Drill Hole USW G-2								
280	Calcite	0.500 ±0.010	1.032 ±0.015	12.0 ±2.4	1.023 ±0.041	>400	−8.35	+19.21
302	Calcite	..	..	..	..	..	−7.90	+19.31
346.7	Calcite	0.405 ±0.008	1.167 ±0.018	4.29 ±0.21	0.915 ±0.037	190 ± 20***	−7.43	+18.22
	Residue	6.85 ±0.14	1.135 ±0.017	2.43 ±0.10	0.965 ±0.049	n.a.	..	..
346.8	Calcite	..	..	..	..	..	−7.37	+18.30
	Opal	..	..	..	..	..	..	+24.8
348.7	Calcite	0.073 ±0.006	1.02 ±0.03	4.6 ±0.5	0.73 ±0.06	142±30†††	−7.47	+18.19
348.8-A§	Calcite	0.136 ±0.004	0.937 ±0.028	10.7 ±1.6	1.010 ±0.040	>400	−6.93	+18.13
348.8-B§	Calcite	33.3 ±0.7	1.026 ±0.015	94 ±15	0.930 ±0.037	280 ± 70	..	..
	U Opal	57.8 ±1.2	1.031 ±0.015	232 ±34	1.027 ±0.031	>400	..	..
359-A	Calcite	1.21 ±0.06	1.020 ±0.015	261 ±80	0.795 ±0.032	170 ± 18	−6.82	+17.98
359-B	Calcite	0.644 ±0.013	0.965 ±0.014	36 ±11	0.811 ±0.032	185 ± 18	..	..
	U Opal	27.0 ±0.5	1.068 ±0.016	234 ±70	1.04 ±0.04	>400	..	..
361	Calcite	..	..	..	..	..	−6.56	+17.77
Drill Hole USW G-3/GU-3								
63	Calcite	0.558 ±0.011	2.26 ±0.03	35 ±4	1.00 ±0.03	227 ± 20	−7.06	+20.23
	Residue	0.66 ±0.04	1.37 ±0.10	7.6 ±1.5	1.94 ±0.19	n.a.	..	..
131	Calcite	3.02 ±0.06	1.43 ±0.02	84 ±40	0.216 ±0.009	26 ± 2	−5.11	+20.16
	U Opal	35.0 ±0.7	1.13 ±0.02	473 ±190	1.15 ±0.05	>400	..	..
147	Calcite	..	..	..	..	..	−5.58	+20.04
159	Calcite	..	..	..	..	..	−5.44	+20.28
318	Calcite	0.0836 ±0.0017	0.991 ±0.020	2.58 ±0.13	1.10 ±0.06	>400	−5.10	+19.11
	Residue	1.88 ±0.11	0.73 ±0.07	4.89 ±0.73	1.27 ±0.13	n.a.	..	..
331	Calcite	0.36 ±0.01	1.06 ±0.04	10 ±5	0.24 ±0.02	30 ± 4	−4.54	+18.73
	U Opal	14.9 ±0.4	1.05 ±0.03	153 ±61	1.13 ±0.06	>400	..	..

*^{230}Th age; calculated using half-lives of ^{230}Th and ^{234}U of 75,200 and 244,000 yr, respectively.
†Sample is below the present water table.
§Sampled from two distinct fracture surfaces at this depth.
**Reported previously by Szabo and others (1981). All ppm U results (except fault gouge and acid-insoluble residues) are given as CaO in the 1981 paper; therefore, ppm U as $CaCO_3$ = ppm U as CaO × 0.56.
††Isochron-plot age, corrected using analytical data of 87-m fault gouge for the 34-m calcite sample; the reported age is considered an age estimate only.
§§Age was inaccurately reported by Szabo and others (1981) as >400 ka.
***Isochron-plot age, corrected using analytical data of both acid-soluble carbonate and acid-insoluble residue.
†††Not corrected for possible initial Th contamination due to small sample size; reported age may be slightly overestimated.
Note: n.a. = not applicable. .. = not determined.

From:

Whelan, J.F., and Stuckless, J.S. 1992. Paleohydrologic implications of the stable isotopic composition of secondary calcite within the Tertiary volcanic rocks of Yucca Mountain, Nevada. IHLRWM 1992. Table 1, p. 1575.

Table 1.

$\delta^{13}C$ and $\delta^{18}O$ values of calcite sampled from drill core (drill hole prefixes USW and UE25 are not shown to save space). Data from Szabo and Kyser[6] and unpublished data from B. A. Carlos (LANL) are also tabulated. Vein, lithophysal cavity (vug), and replacement cement calcite occurrences are distinguished (occurrence type data was not available for the data from Szabo and Kyser[6]).

Sample #	Drill Hole	Depth (m)	Type[a]	$\delta^{13}C$[b]	$\delta^{18}O$[c]
HD-280	G-1	885	vein	-9.5	14.2
HD-281	G-1	895	vein	2.3	11.0
	G-2[d]	280		-8.4	19.2
	G-2[d]	302		-7.9	19.3
	G-2[d]	347		-7.4	18.2
	G-2[d]	347		-7.4	18.3
	G-2[d]	349		-7.5	18.2
	G-2[d]	349		-6.9	18.1
	G-2[d]	359		-6.8	18.0
HD-272A	G-2	441	vug	-5.7	14.7
HD-272B	G-2	"	vug	-8.3	15.6
HD-272D	G-2	"	vein	-3.6	14.5
HD-273A	G-2	464	vug 1	-4.2	14.7
HD-273B	G-2	"	vug 2	-7.9	17.3
HD-273C	G-2	"	vug 3	-6.0	15.1
HD-273D	G-2	"	vug 4	-7.9	17.1
HD-273E	G-2	"	vein 1	-6.9	15.5
HD-273F	G-2	"	vein 2	-7.3	15.7
HD-274A	G-2	476	vug 1	-1.5	14.4
HD-274B	G-2	"	vug 2	-0.9	13.8
HD-274C	G-2	"	vug 3	-4.7	15.9
HD-274D	G-2	"	vug 4	-7.6	18.3
HD-274E	G-2	"	vug 5	-8.2	18.3
HD-275B	G-2	477	vug 2	-2.0	14.8
HD-275C	G-2	"	vug 3	-0.3	14.0
HD-261A	G-2	1280	vein	0.0	4.2
HD-261B	G-2	"	cement	-0.6	7.8
HD-262A	G-2	1459	vein	-1.5	7.8
HD-262B	G-2	"	cement	-1.0	8.1
HD-263A	G-2	1637	vein	1.0	9.4
HD-263B	G-2	"	cement	0.4	7.8
HD-264A	G-2	1640	vein 1	1.9	12.9
HD-264B	G-2	"	vein 2	0.7	6.2
HD-264C	G-2	"	cement	-0.4	8.9
HD-265A	G-2	1756	vein 1	-0.4	8.6
HD-265B	G-2	"	vein 2	-0.8	7.1
HD-265C	G-2	"	cement	-0.5	9.7
HD-266A	G-2	1794	cement	1.3	10.5
	G-3[d]	63		-7.1	20.2
	G-3[d]	131		-5.1	20.2
	G-3[d]	147		-5.6	20.0
	G-3[d]	159		-5.4	20.3
HD-276A	GU-3	295	vein?	-4.0	18.7
HD-276B	GU-3	"	vein?	-5.2	19.2
HD-277A	GU-3	296	vein	-5.4	19.4
HD-267A	G-3	313	vein 1	-4.3	18.9
HD-267B	G-3	"	vein 2	-4.8	19.2
	G-3[d]	318		-5.1	19.1
	G-3[d]	331		-4.5	18.7
HD-278A	GU-3	347	vein 1	-5.7	18.9
HD-278B	GU-3	"	vein 2	-6.3	19.0
HD-278C	GU-3	"	veinlet 3	-6.5	19.1
HD-279A	GU-3	358	vein 1	-6.0	18.9
HD-279B	GU-3	"	vein 2	-5.7	19.4
HD-268A	G-3	1310	vein	2.2	10.9
HD-268B	G-3	"	vein	2.1	10.6
HD-268C	G-3	"	vein	2.4	11.3
HD-268D	G-3	"	vein	2.3	9.5
HD-269A	G-3	1346	vein 1	0.5	9.7
HD-269B	G-3	"	vein 2	-2.0	11.7
HD-270A	G-3	1464	vein	1.7	7.5
HD-255A	b1	942	vein	3.8	5.3
HD-256A	b1	953	vein A	2.4	5.8
HD-256B	b1	"	vein B	1.8	5.8
HD-257A	b1	971	vein 1	4.2	11.7
HD-257B	b1	"	vein 2	4.4	11.4
HD-258A	b1	1098	vein	2.0	6.0
HD-259A	b1	1116	vein 1	1.6	5.7
HD-259B	b1	"	vein 2	0.6	4.4
HD-259C	b1	"	cement	2.1	6.8
HD-260A	b1	1216	vein 1	1.3	5.5
HD-260B	b1	"	vein 2	2.1	4.6
HD-260C	b1	"	cement	1.0	8.8
	G-4[e]	77		-6.8	17.0
HD-674A	G-4	108	vug 1	4.9	16.0
HD-674B	G-4	"	vug 2	0.6	16.5
HD-679A	G-4	265	vug 1	-7.1	16.8
HD-679B	G-4	"	vug 2	-1.2	14.7
	G-4[e]	"		-0.8	14.1
	G-4[e]	353		-3.6	17.1
HD-681A	G-4	401	vein	-9.1	16.0
	G-4[e]	"		-9.0	15.2
	G-4[e]	587		-6.7	17.4
	G-4[e]	663		-7.9	17.6
HD-687A	G-4	810	vein	-8.2	13.6
	G-4[e]	"		-8.0	13.1
HD-689A	G-4	842	vein	-5.7	13.3
	G-4[e]	"		-6.4	13.2
HD-271A	p1	1197	Pz ls	1.2	10.3

a - numbered sequences are from early to late.
b - d13C vs.PDB.
c - d18O vs. SMOW.
d - analyses reported by Szabo and Kyser6.
e - unpublished data from B.A. Carlos.

carbonates suggesting diagenetic ^{18}O-depletion.

Figure 4 shows the $\delta^{13}C$ of calcite samples from USW G-2 against lithology. This plot illustrates the typically low $\delta^{13}C$ values of calcite in the UZ and the much higher values of the SZ and the control of calcite distribution by lithology and alteration: macroscopic calcite generally comes from fracture coatings or fillings in welded units, in lithophysal cavities, or in alteration zone IV.

6-2-95 JF

FROM:
Whelan, J.F., etal. 1994. Paleoclimatic and paleohydrologic records from secondary calcite: Yucca Mountain, Nevada. IHLRWM 1994. Table 1, p.2741.

JF

Table 1: $\delta^{18}O$ values and formation temperatures of secondary opal

SAMPLE #	BORE HOLE	DEPTH (m)	$\delta^{18}O_{smow}$	δDH_2O^* = -10.5	δDH_2O^* = -13
HD-351B	USW G-2	92.2	26.6	18	10
HD-355A	USW G-2	236.7	20.7	42	31
HD-355A	USW G-2	236.7	20.5	43	32
HD-356A	USW G-2	240.7	21.7	37	27
HD-358A	USW G-2	257.8	24.1	28	18
HD-362A	USW G-2	280.2	21.2	39	29
HD-700A	USW G-4	74.2	24.1	28	18
HD-306C	UE25 a#1	253.0	18.6	51	40
HD-926A	UE25 a#5	85.2	21.9	36	26
HD-929A	UE25 a#5	92.2	26.6	18	10

* - calculated formation temperatures from waters with δDH_2O values -10.5 and -13 ‰.

6-29-95 JF

FROM:

Yang, I.C. 1992. Flow and transport through unsaturated rock: Data from two test holes, Yucca Mountain, Nevada. IHLRWM 1992. Table 1, p. 735.

Table 1. Tritium concentrations of pore water in core samples from test holes UE-25 UZ #4 and UE-25 UZ #5

[m, meters; TU, tritium unit]

Sample ident. No., UE-25	Depth interval (m)	Date of Coll.	Tritium conc. (TU)
UZ4-D-T-1	1.0 - 2.3	10-01-84	19 ± 5
UZ4-D-T-2	2.5 - 4.5	10-01-84	22 ± 5
UZ4-D-T-3	5.5 - 6.5	10-01-84	7 ± 5
UZ4-D-T-4	8.8 - 10.3	10-01-84	2 ± 5
UZ4-D-T-5	11.0 - 11.8	10-01-84	3 ± 5
UZ4-CF-25	24.7 - 24.8	10-02-84	28 ± 5
UZ4-CF-24	25.5 - 25.6	10-02-84	3 ± 4
UZ4-D-TP-8	33.5 - 33.6	10-02-84	22 ± 5
UZ4-D-3	41.8 - 41.9	10-02-84	24 ± 5
UZ4-D-4	44.8 - 44.9	10-02-84	41 ± 5
UZ4-D-6	44.9 - 45.0	10-02-84	38 ± 4
UZ4-D-5	46.3 - 47.9	10-02-84	45 ± 5
UZ4-D-TP-10	49.4 - 49.5	10-02-84	45 ± 6
UZ4-TP-6	95.6 - 95.7	10-05-84	0 ± 4
UZ5-D-1	28.3 - 28.4	11-01-84	60 ± 4
UZ5-D-2	28.8 - 28.9	11-01-84	49 ± 4
UZ5-CF-51	29.8 - 30.0	11-01-84	65 ± 5
UZ5-D-TP-3	30.4 - 30.6	11-01-84	51 ± 4
UZ5-D-4	31.4 - 31.5	11-01-84	11 ± 5
UZ5-D-TP-12	32.6 - 32.8	11-01-84	75 ± 5
UZ5-D-5	33.6 - 33.7	11-02-84	39 ± 5
UZ5-D-6	34.0 - 34.1	11-02-91	22 ± 5
UZ5-D-7	34.8 - 34.9	11-02-84	42 ± 4
UZ5-D-8	36.0 - 36.1	11-02-84	66 ± 4
UZ5-D-9	36.5 - 36.6	11-02-84	15 ± 4
UZ5-D-10	36.6 - 36.7	11-02-84	36 ± 4
UZ5-D-11	37.2 - 37.3	11-02-84	4 ± 5
UZ5-D-TP-32	37.6 - 37.7	11-02-84	13 ± 7
UZ5-D-TP-19	44.8 - 44.9	11-02-84	6 ± 4
UZ5-D-15	68.6 - 68.8	11-06-84	10 ± 4
UZ5-D-16	70.1 - 70.2	11-06-84	1 ± 4
UZ5-D-TP-22	72.4 - 72.5	11-06-84	0 ± 4
UZ5-D-TP-23	72.5 - 72.7	11-06-84	7 ± 4
UZ5-D-TP-24	75.3 - 75.5	11-07-84	0 ± 4
UZ5-D-18	78.7 - 78.9	11-07-84	0 ± 4
UZ5-D-19	82.4 - 82.6	11-07-84	4 ± 4
UZ5-D-TP-29	90.1 - 90.2	11-08-84	1 ± 4
UZ5-TP-9	94.1 - 94.3	11-08-84	6 ± 5
UZ5-TP-10	94.3 - 94.5	11-08-84	0 ± 4
UZ5-D-21	98.3 - 98.4	11-08-84	1 ± 4

FROM: Yang, I.C., etal. 1988. Triaxial-Compression Extraction of Pore Water from Unsaturated Tuff, Yucca Mountain, Nevada. USGS Water-Resources Investigations Report 88-4189. Table 3, pp.33-34.

Table 3.--*Chemical composition of extracted pore water*

[Depth is distance from land surface to top of core-sample interval; --, data not available; <, less than]

Sample number (depth in meters)	Stress (megapascals)		Major ions (milligrams per liter)							Minor ions (micrograms per liter)			
	Axial	Confining	Ca	Mg	Na	K	Si	Cl	SO_4	Fe	Mn	Sr	Zn
UZ5-TP-4	83	62	56	12	38	12	97	--	--	118	37	546	26
(31.6)	117	62	58	12	33	9	99	34	39	74	20	559	34
(Trial #10)	138	62	61	12	30	15	99	--	--	127	21	585	140
UZ5-TP-1 and -3	76	59	36	7	28	7	72	42	41	<3	7	--	--
(30)	125	62	48	10	29	7	88	45	41	24	11	--	--
(Trial #41)													
UZ5-TP-6 and -5	90	62	27	5	26	6	100	41	37	100	10	--	--
(36)	152	62	27	6	35	8	97	43	47	22	15	--	--
(Trial #56 & #58)													
UZ5-TP-9 and -8	76	59	78	16	61	--	89	89	--	18	43	--	--
(94)	128	62	36	7	39	--	94	51	41	<.1	.3	.5	48
(Trial #15 & #38)													
UZ5-TP-14 and -15	97	62	49	11	58	5	92	83	90	35	4	--	--
(97)	152	62	63	13	54	--	89	--	--	5	21	--	--
(Trial #31 & #35)													
UZ4-TP-1	62	52	116	19	60	13	82	91	155	6	35	1,357	17
(91.6)	83	59	108	19	64	10	87	90	154	11	13	1,366	<3
(Trial #16)	138	62	116	19	64	13	89	92	154	9	62	1,399	14
	[1]178	64	100	19	70	14	90	101	161	11	17	1,325	9
UZ4-TP-2	62	52	127	21	65	15	88	105	174	5	57	1,504	25
(91.3)	138	59	122	20	69	16	88	106	172	5	73	1,502	18
(Trial #17)	[1]178	64	100	19	70	14	90	101	161	11	17	1,325	9
UZ4-TP-3	48	41	123	20	60	14	82	100	164	6	69	1,409	15
(91.4)	138	62	122	20	64	16	92	97	163	4	50	1,450	9
(Trial #18)	[1]178	64	100	19	70	14	90	101	161	11	17	1,325	9

Table 3.--*Chemical composition of extracted pore water*--Continued

Sample number (depth in meters)	Stress (megapascals)		Major ions (milligrams per liter)							Minor ions (micrograms per liter)			
	Axial	Confining	Ca	Mg	Na	K	Si	Cl	SO_4	Fe	Mn	Sr	Zn
UZ4-TP-4	41	34	105	18	64	15	83	84	146	6	56	1,248	3
(91.5)	110	59	107	18	68	16	93	87	149	11	65	1,302	19
(Trial #19)	[1]138	59	101	18	70	14	96	91	151	5	29	1,276	4
UZ4-TP-5	83	59	67	12	43	14	86	78	123	85	13	863	9
(95.3)	[1]117	66	71	13	40	14	85	92	147	86	21	892	71
(Trial #21)													
UZ4-TP-6	83	59	74	13	47	15	83	99	127	60	24	931	107
(95.6)	[1]117	66	71	13	40	14	85	92	147	86	21	892	71
(Trial #22)													

[1]Two or three water samples (from the same stress level) were combined to provide sufficient water volume for chemical analysis.

NOTE: Core from drill hole UE-25 UZ #4 may have been exposed to evaporation; chemical concentrations may be increased.

June 9, 1995 TLT

May 26, 1995
Timothy L. Tolley

Using values for matrix air-entry parameters ($alpha_{VG}$) and matrix saturation/desaturation parameters ($beta_{VG}$), (from "Total-System Performance Assessment for Yucca Mountain-SNL Second Iteration (TSPA-1993)" volume 1, tables 7.5 and 7.6), values for saturation levels [S(h)] and relative hydraulic conductivities (K_r) were calculated using the Van Genuchten equations:

$S(h)=[1=(-alpha_{VG}h)^{beta}]^{-m}$

$K_r(s)=sqrt(S)[1-(1-S^{(1/m)})^m]^2$

h=hydraulic head

m=1-(1/m)

These calculations were made at levels of h from 0 meters to -400 meters. The values of S to h and K_r to h were then graphed. The calculations and the graphs were done on AXUM spreadsheet.

June 8, 1995
Timothy L. Tolley

The beta function in the previous version of the Latin Hypercube Sampling program (LHS) was not functional and as it seems that it will be needed to estimate the likelihood of perched zones of saturation forming. Initially, a code was written with Matlab 4.2 that varied the standard deviation and mean of a normal distribution function so that it approximated the beta function. Since then an updated version of LHS program, (LHS94), has been obtained and this is currently being tested for its beta function capability.

6-10-95 JF

QA NOTED IN SOURCES USED FOR DATA

Benson, L.V., and McKinley, P.W. 1985. Chemical Composition of Ground Water in the Yucca Mountain Area, Nevada, 1971-1984. USGS Open-File Report 85-484.
QA procedures not noted.

Carlos, B.A. 1987. Minerals in Fractures of the Saturated Zone from Drill Core USW G-4, Yucca Mountain, Nye County, Nevada. Los Alamos National Laboratory LA-10927-MS.
QA procedures not noted.

Fabryka-Martin, J.T., Wightman, S.J., Murphy, W.J., Wickham, M.P., Caffee, M.W., Nimz, G.J., Southon, J.R., Sharma, P. 1993. Distribution of Chlorine-36 in the unsaturated zone at Yucca Mountain: An indicator of fast transport paths. Conference Proceedings FOCUS '93: Site Characterization and Model Validation: 58-68.
QA procedures not noted.

JF Mower, T.E., Higgins, J.D., Yang, I.C., and Peters, C.A. 1994. Pore-Water Extraction from Unsaturated Tuff by Triaxial and One-Dimensional Compression Methods, Nevada Test Site, Nevada. USGS Water-Resources Investigations Report 93-4144.
QA procedures not noted.

Szabo, B.J., and Kyser, T.K. 1990. Ages and stable-isotope composition of secondary calcite & opal in drill cores from Tertiary rocks of the Yucca Mountain area, Nevada. Geological Society of America Bulletin 102(12): 1714-1719.
QA procedures not noted. Samples provided by U.S.G.S.

Whelan, J.F., and Stuckless, J.S. 1992. Paleohydrologic implications of the stable isotopic composition of secondary calcite within the Tertiary volcanic rocks of Yucca Mountain, Nevada. High-Level Radioactive Waste Management. Proceedings of the Third International Conference: 1572-1581.
QA procedures not noted.

Whelan, J.F., Vaniman, D.T., Stuckless, J.S., and Moscati, R.J. 1994. Paleoclimatic and paleohydrologic records from secondary calcite: Yucca Mountain, Nevada. High-Level Radioactive Waste Management. Proceedings of the Fifth International Conference: 2738-2745.
QA procedures not noted.

6-10-95 JF

QA NOTED IN SOURCES USED FOR DATA (continued)

Yang, I.C. 1992. Flow and transport through unsaturated rock. Data from two test holes, Yucca Mountain, Nevada. High-Level Radioactive Waste Management. Proceedings of the Third International Conference: 732-737.
QA procedures not noted.

Yang, I.C., Turner, A.K., Sayre, T.M., and Montazer, P. 1988. Triaxial-Compression Extraction of Pore Water from Unsaturated Tuff, Yucca Mountain, Nevada. USGS Water-Resources Investigations Report 88-4189.
QA procedures not noted.

JF Bish, D.L., and Chipera, S.J. 1989. Revised Mineralogic Summary of Yucca Mountain, Nevada. Los Alamos National Laboratory LA-11497-MS..
QA procedures not noted.

Chipera, S.J., and Bish, D.L. 1989a. Quantitative X-Ray Diffraction Analyses of Samples used for Sorption Studies by the Isotope and Nuclear Chemistry Division, Los Alamos National Laboratory. Los Alamos National Laboratory LA-11669-MS.
QA Level III noted in Appendix II, page 19.

Chipera, S.J., and Bish, D.L. 1989b. The Occurrence and Distribution of Erionite at Yucca Mountain, Nevada. Los Alamos National Laboratory LA-11663-MS.
QA Level III noted in Appendix I, page 20.

8/26/95
DB

3–D Geologic Framework Model of Yucca Mountain Subregion

Stirewalt et al. (1994) & (1995)

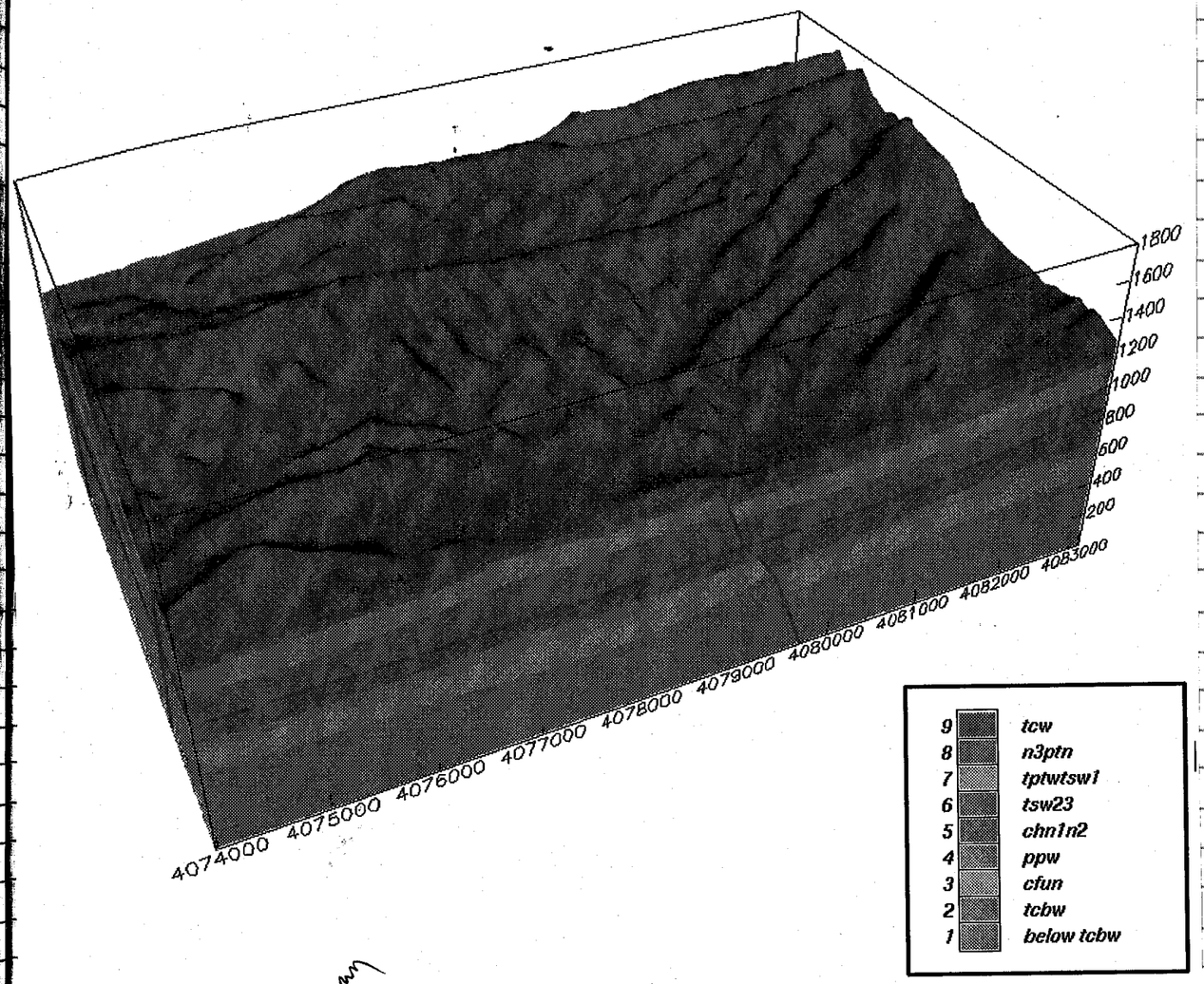

DB Johnson

8/25/95
DRD

Geochemical Information – Yucca Mountain Subregion

Wells in YM subregion for which geochemical data are available includes:

- Mineralogy
- Stable Isotope Chem
- ^{36}Cl
- Water Chem

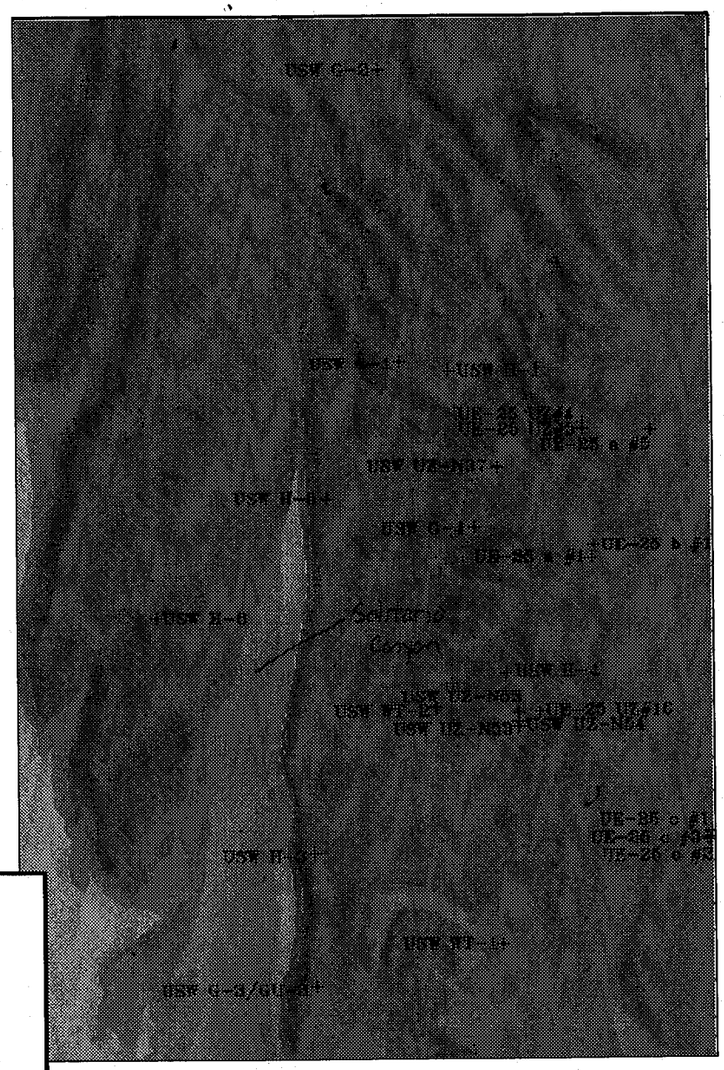

9	tcw
8	n3ptn
7	tptwtsw1
6	tsw23
5	chn1n2
4	ppw
3	cfun
2	tcbw
1	below tcbw

Transect Through G–2, G–1, G–4, and G–3/GU–3 Boreholes

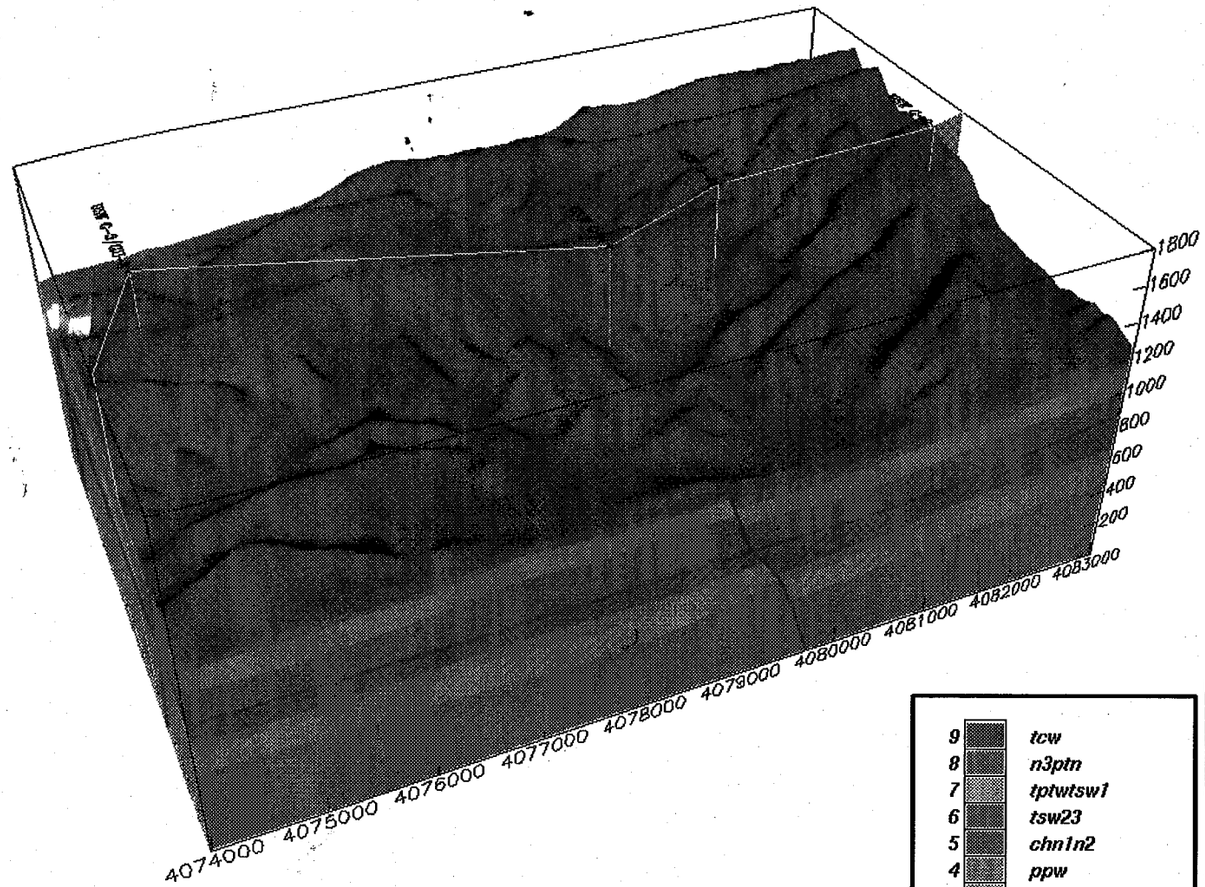

9	tcw
8	n3ptn
7	tptwtsw1
6	tsw23
5	chn1n2
4	ppw
3	cfun
2	tcbw
1	below tcbw

8/25/95
DRJ

Cross-Section based on Transect shown p. 21 of this volume

N-S Cross-Section Looking East

8/25/95
DRJ

$\delta^{18}O$ for calcite in wells G1, G-2, G-3 & G-4

N-S Cross-Section - Oxygen-18 (o/oo)

8/25/95
DBL

D.R. Lumm

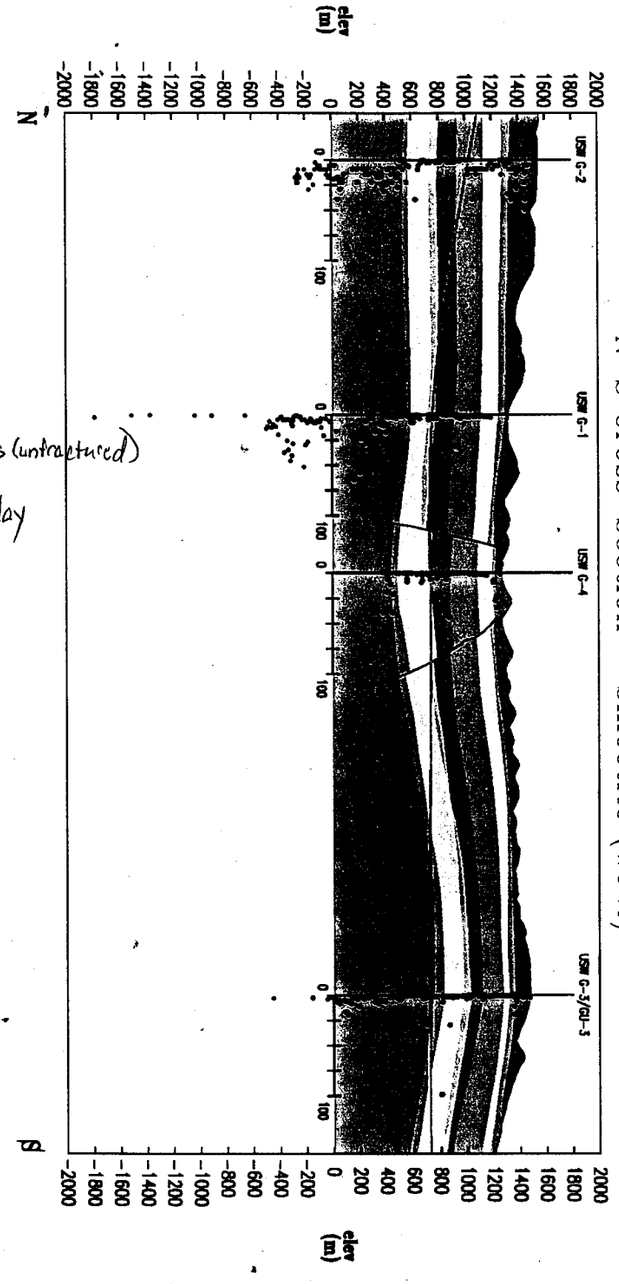

N–S Cross-Section – Smectite (Wt %)

Note:

1) Increase in clay to north (closer to Timber Mtn caldera)

2) Higher clay content in welded (fractured) tuffs. Non-welded units (unfractured) acted as impermeable caps to flow during clay formation.

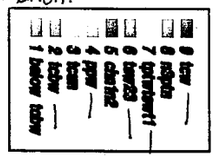

12/7/95
Entries composed by T. Tolley, entered here by D.R. Lumm

D.R. Lumm

Overview

For this preliminary study a code was written in Matlab 4.2 to give a first estimate of the likely areas for trapping to occur. Some of the things taken into account in this code were: 1) variability of the hydraulic conductivity due to the heterogeneity of the rock units 2) change of hydraulic conductivity due to varying levels of saturation 3) the vertical arrangement of the beds 4) the difference in hydraulic conductivity that may cause trapping 5) effects of different layers being subjected to different suction levels and different levels of saturation. Some important considerations that are left for later phases of this study are: 1) variability of the bed thicknesses (and thus the variability of the depths to the interfaces at different locations) 2) the effects and location of faulting 3) variability of the matrix air entry parameters or the matrix saturation/desaturation parameters 4) effects on the area directly around the saturated zone

The first step performed by the code is to load the data on the mean saturated hydraulic conductivity, in log to the base ten form, (LK_{sat}), standard deviation of LK_{sat}, mean depth from the ground surface to the interfaces between the layers, mean alpha (matrix air-entry parameter) and mean beta (matrix saturation/desaturartion parameter). Alpha and beta are parameters that define the shape of the probability distribution function given by the Van Genuchten

12/7/95
T. Tolley +
D.P. Lumm

equations.

Next a series of random LK_{sat} values was generated by Matlab for each layer based on the mean LK_{sat}, its standard deviation and a normal distribution. This provided values for LK_{sat} that covered its entire range of possible values Figure 1b. Each of the random LK_{sat} values were converted to K_{sat} by taking the antilog of LK_{sat}.

The next several steps were performed stepwise for each of the suction levels being considered. Using the Van Genuchten equations the values for **unsaturated** hydraulic conductivity, K_{unsat}, were determined for each of the random K_{sat} values for each layer. The log to the base ten was taken of each of these K_{unsat} values giving LK_{unsat} values. All of the LK_{unsat} values for each unit were compared with the corresponding LK_{unsat} values of the rock unit directly beneith it. If the difference in the LK_{unsat} values was greater than a user specified tolerance, and the unit with the smaller (most negative) LK_{unsat} value was the lower of the two units, then a potential exist for a perched water body to form. The number of times that this trapping potential occurred for a specific interface relative to the total number of random samples indicates the likelihood that a trap could form at that interface for that suction level somewhere in the area. For example, the number of random Monte Carlo (nmc) samples was 200 for each layer in this case, and if the difference between each of the 200 random Monte Carlo LK_{unsat} values for unit 1 and the corresponding random Monte Carlo LK_{unsat} values for unit 2 was greater than the user specified tolerance for only 50 of those 200 instances then the trapping potential would be 50/200 or 25%.

D.P. Lumm

12/7/95
T. Tolley
+ D.P. Lumm

These steps were repeated for the next suction level until the maximum suction level is reached.

In order to achieve a more realistic representation of the suction levels at each interface, the water table was considered to be at the level of interface 5, the lowest interface considered. The suction level at each interface was determined by subtracting the depth to the interface from the depth to the water table. This produced suction levels for interfaces 1 through 5 of -704, -665, -351, -160, and 0 respectively. The Matlab code was run for each of these suction levels and the trapping potential of each suction level was applied to its respective interface.

Testing

In testing the code, a difference of "2" for the $\log_{10}$ of the hydraulic conductivity, (log K), was used and the suction level varied from h=0 to -30 meters in increments of -10 meters (h=0,-10,-20,-30). The values for depth, K_{sat}, log K_{sat}, alpha, beta and standard deviation were taken from the TSPA (1993).

The first step in the code is to calculate for each layer the saturation, relative K, (K_{rel}), and hydraulic conductivity at less than saturation (K_{unsat}). For the first suction level (h=0), K_{unsat} is equal to K_{sat}. The Van Genuchten equations are used for this procedure:

$$\text{saturation} = (1+(-\text{alpha}*h)^{\text{beta}})^{-m} \qquad \text{where } m=1-(1/\text{beta})$$

$$K_{rel}=\text{sqrt}(\text{saturation})*(1-(1-\text{saturation}^{(1/m)})^{m})^{2}$$

$$K_{unsat}=K_{sat}*K_{rel}$$

12/7/95
T. Tolley +
D.R. Turney

The $\log_{10}$ values of the K_{unsat} of each layer was then calculated. All of the above values were displayed as they were calculated so that the accuracy of each step could be confirmed by hand calculations.

Next many random values for the log K_{unsat} were chosen by adding to their mean log K_{unsat}, the standard deviation times three times a random number between -.5 and .5 (random number chosen by Matlab). This produces a potential value for the log K within three standard deviations of the mean (i.e. 99% of all possible values).

Each of these random values for log K is subtracted from the corresponding log K value for the rock unit directly beneith it. This is done for all the layers of rock (except of course the bottom layer). Whenever a difference in the log K values excedes the predetermined 'tolerance', and the lesser value (most negative) is the lower unit of the two, a potential exist for a trap to form at the intersection between these two layers. The number of times that this occurs for a given interface gives an indication of the probability of a trap forming at that interface. The results are then plotted in the form of a vertical axis for depth and a horizontal axis for probability of a potential trap.

This entire process is repeated for each of the levels of suction (0, -10, -20, -30 meters in the test case).

D.R. Turney

12/7/95
T. Tolley
D.R. Turney

Data

The data used in this study was taken from the Sandia Report, SAND93-2675, Yucca Mountain Site Characteristic Project, Total-System Performance Assessment for Yucca Mountain-SNL Second Iteration (TSPA-1993). TSPA-1993 divides Yucca Mountain into ten hydrgeologic units, (Table 7-2, page 7.9). Because the current Center for Nuclear Waste Regulatory Analysis, (CNWRA), model of Yucca Mountain is divided slightly differently some modifications were made to the TSPA-1993 division. The correlation between these two divisions is shown below:

unit#	TSPA-1993	unit#	Current Study
1	Tiva Canyon welded	1	Tiva Canyon welded
2	Paintbrush nonwelded	2	Paintbrush nonwelded
3	Topopah Spring	3	Topopah Spring
4	Topopah Spring Vitrophyre		
5	Calico Hills/Prow Pass nonwelded-vitric	4	Calico Hills
6	Calico Hills/Prow Pass nonwelded-zeolitic		
7	Prow Pass welded	5	Prow Pass welded
8	Bullfrog welded	6	Bullfrog welded
9	Bullfrog nonwelded		
10	Tram		

D.R. Turney

12/7/95
T. Tolley *
D.R. Wilmer

The Tiva Canyon welded and Paintbrush nonwelded units translate directly. The current CNWRA model has Topopah Spring divided into units according to their properties, Topopah Spring 1 and Topopah Spring 2&3; but it does not recognize the Topopah Spring vitrophyre. The TSPA-1993 divides Topopah Spring into Topopah Spring welded (composite and repository) and Topopah Spring vitrophyre. Since the Topopah Spring vitrophyre is not recognized by the current CNWRA model and it is not continuous over the entire study area, it is ignored in this study (except with consideration to its mean thickness which is included in the total thickness of the Topopah Spring unit). This study then considers Topopah Spring as one unit. Both the Calico Hills/Prow Pass nonwelded vitric and Calico Hills/Prow Pass nonwelded zeolitic are recognized by the TSPA-1993 but are combined into the single Calico Hills nonwelded recognized by the CNWRA model. Prow Pass welded and Bullfrog welded correlate directly and are thus unchanged. Since the Bullfrog nonwelded and Tram occur only in the saturated zone, (TSPA-1993, p.7.9), they are not included in this study of perched water bodies. The above correlation leaves six units to be evaluated.

This arrangement of hydrogeologic units must of course be accompanied by similar changes in the corresponding data. The LK_{sat} values and their coefficient of variation, (cv), for units 1, 3, 5 and 6, (Tiva Canyon, Topopah Spring, Prow Pass welded and Bullfrog welded respectively), were taken from Table 7-5b in TSPA-1993. Unit 2, Paintbrush Tuff, has a bimodal distribution (Figure 7-5) with each mode listed seperately in Table 7-5b of TSPA-1993. Table 7-5a

D.R. Wilmer

- sebastian/ttolley

files Kun6.m
param6.m
para_inp.m

12/7/95
T. Tolley *
D.R. Wilmer

of TSPA-1993 does not seperate unit 2 and since the TSPA-1993 does not specify if the bimodal character is a result of lateral variations of the properties or because unit 2 should divided into two units, the single unit values for LK_{sat} and cv from Table 7-5a were used. For unit 4, Calico Hills, (vitric and zeolitic units), a weighted average of the K_{sat}'s, (antilogs of LK_{sat} values given in table 7-5b, TSPA-1993:), were calculated based on the thicknesses of each unit (Table 7-2, TSPA-1993).

thickness CH_{vitric} = 63.99 meters

thickness $CH_{zeolitic}$ = 126.88 meters

The mean K_{sat} for the two units combined was calculated as follows:

mean K_{sat} = (mean $K_{sat,vitric}$) * (thickness CH_{vitric} / thickness CH_{total}) + (mean $K_{sat,zeolitic}$) * (thickness $CH_{zeolitic}$ / thickness$_{total}$)

mean $LK_{sat} = \log_{10}(\text{mean}K_{sat})$

To find the standard deviation (SD) of the SD of each unit the equation SD = CV*abs(mean LK_{sat}) was used . For unit #4 (Calico Hills) the standard deviation was first calculated for the individually for its vitric and zeolitic components. These two individual SD values were then averaged using the same weighted average scheme that was used to calculate the K_{sat} values.

The mean matrix air-entry parameter(alpha) and the mean matrix saturation/desaturation parameter (beta) were taken from TSPA-1993 Table 7-6a and Table 7-7a respectively. For units 1, 2, 3, 5 and 6 (Tiva Canyon, Paintbrush Tuff, Topopah Spring, Prow Pass welded and Bullfrog welded respectively), the values were taken directly from their respective tables. For Calico Hills the combined values were

12/7/95
T. Tolley +
D.R. Lumm

determined by the same weighted average method used for the LK_{sat} values above.

The thicknesses of the units were taken from Table 7-2 of the TSPA-1993. Units #1 and #2, (Tiva Canyon and Paintbrush nonwelded), were taken directly from Table 7-2. The thicknesses of the Topopah Spring welded, (composite and repository), and Topopah Spring vitrophyre from Table 7-2 were added together to give the thickness of unit #3 (Topopah Spring). The thickness of unit #4 (Calico Hills) was taken from the combined thicknesses of Calico Hills nonwelded vitric and Calico Hills nonwelded zeolitic from Table 7-2. The thickness of unit #5 (Prow Pass) was not given so an estimate was made based on information taken from the CNWRA model. The thickness of unit #6 (Bullfrog) was not considered since there were no interfaces below it that were not located in the saturated zone.

The data used for this Matlab code is summarized in the table below:

unit#	mean LK_{sat}	SD_{LKsat}	mean depth	mean alpha	mean beta	mean porosity
1	-10.69	.9087	-81.00	.0218	1.620	.087
2	-7.96	2.409	-120.43	.2485	2.611	.421
3	-10.68	.9292	-434.06	.0299	1.793	.139
4	-9.42	1.0377	-624.93	.0306	2.0866	.314
5	-9.04	.6599	-785	.0180	7.014	.292
6	-9.56	.4684	-	.0299	1.793	.165

12/7/95
T. Tolley +
D.R. Lumm

Results

That the hydraulic conductivity for an individual sample will vary depending upon the level of saturation and that the character of the changing hydraulic conductivity will be unique for each layer is seen in figure 1. For units 5 and 6 this figure shows the maximum and minimum values of the hydraulic conductivity for all the random values at suction heads from 0 meters to 500 meters at 10 meter increments. This figure indicates that initially the hydraulic conductivity of both unit 5 and unit 6 are approximately the same. Up to about 50 meters of suction the hydraulic conductivity of unit 5 remains constant but the hydraulic conductivity of unit 6 begins to decrease immediately. This produces a trapping potential at intersection 5 and this trapping potential is also indicated in Figure 2a-c. After about 50 meters of suction the decreasing hydraulic conductivity of unit 6 begins to level off while the hydraulic conductivity of unit 5 begins to rapidly decrease. By 100 meters of suction the hydraulic conductivities of the two units are about equal again and thus there is no longer a trapping potential at this intersection. This is confirmed by Figure 3d and 3e. 12/7/95

This program was run three times for levels of suction from h=0 to h=1000 meters. For the first run it was assumed that a difference of at least "1" in the values of the log to the base ten of the hydraulic conductivity (LK_{unsat}) of the two layers forming a particular interface was sufficient to cause a potential trap to

12/7/95
T. Talley
+ D.R. Jumm

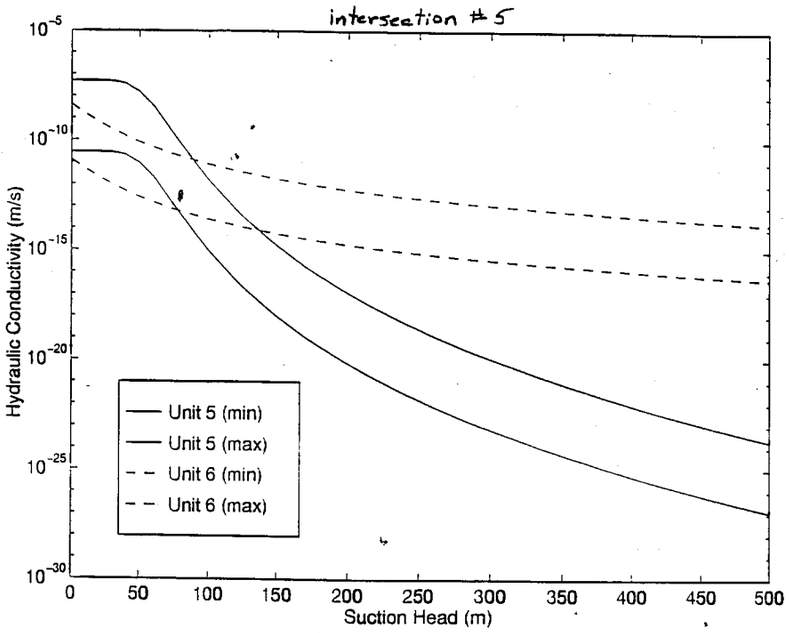

Figure 1

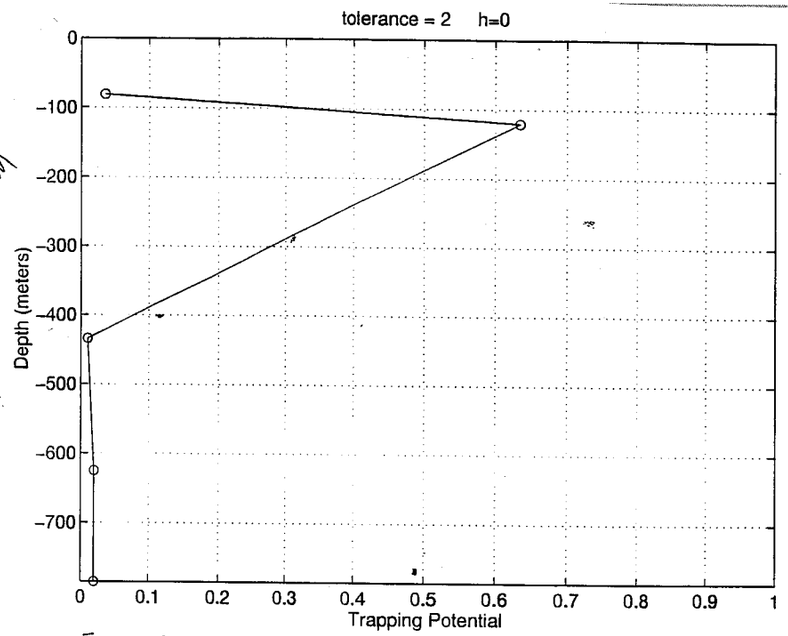

Figure 2a

12/7/95
T. Talley
+ D.R. Jumm

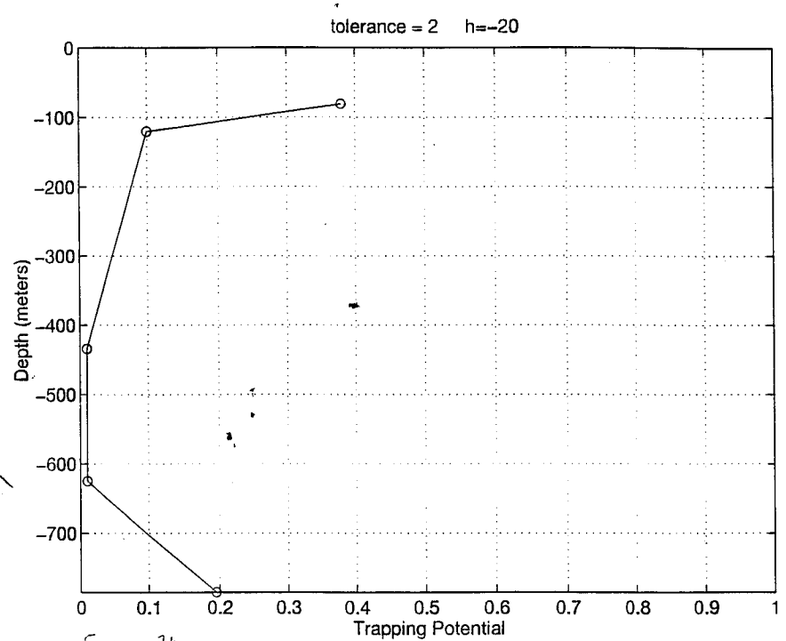

Figure 2b

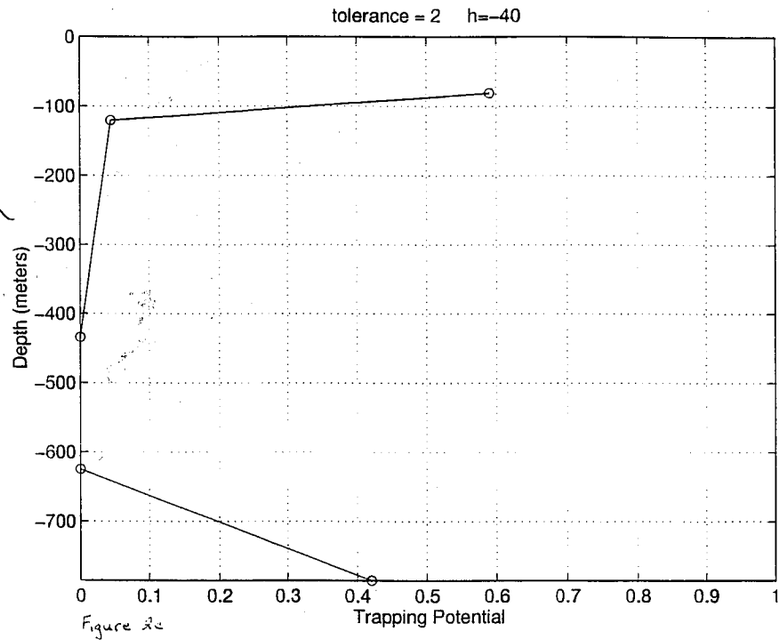

Figure 2c

12/7/95
T. Tolley +
D.P. Jumm

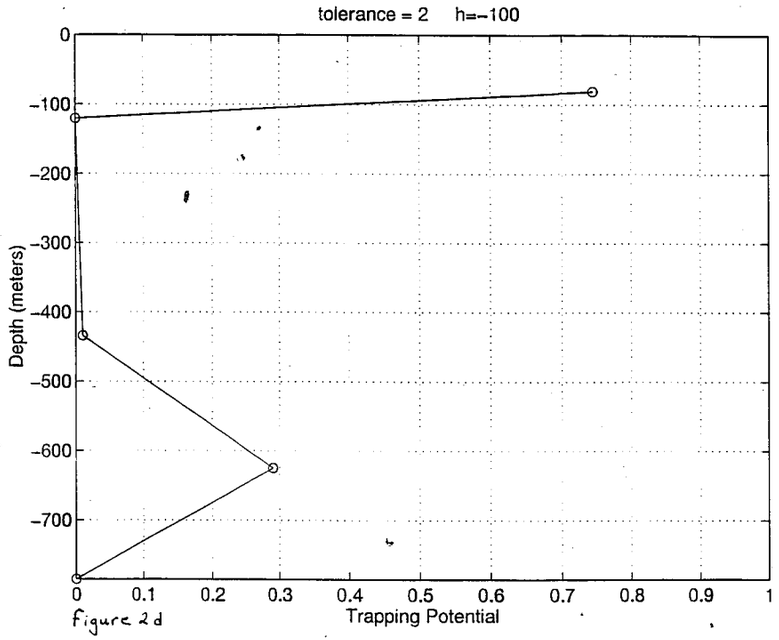

Figure 2d

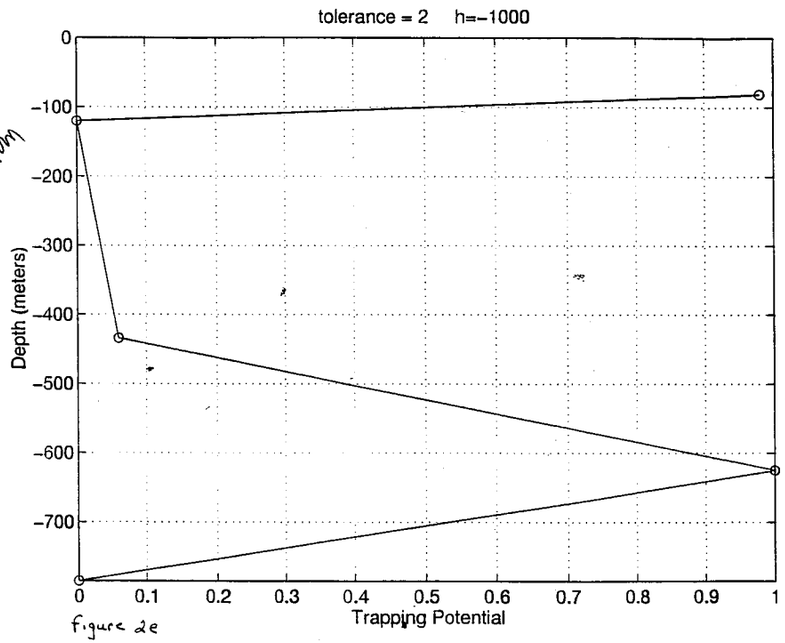

figure 2e

12/7/95
T. Tolley
& D.P. Jumm

form. The second and third runs assumed that a difference of 2 and 3 respectively of the LK_{unsat} values would be necessary to cause a trap to form. Although the individual trapping potential values were all different for the runs of the three different tolerance levels, the overall pattern was essentially the same for all three runs. As would be expected the trapping potential for all interfaces at all values of suction, (h), was generally highest for a tolerance of "1" and lowest for a tolerance of "3".

The overall pattern for all three runs is demonstrated below using the run with a tolerance value of "2". The results of this run can be seen in Figure 2a-e and are summarized in Table 2. Initially interface #2 dominates with a trapping potential of about 64%. With increasing suction this quickly changes and by 40 meters of suction the trapping potential of unit #2 has decreased to about 4% and the trapping potentials of units #1 and #5 have increased from less than 5% to about 59% and 42% respectively. Another change occurs by 100 meters of suction where the trapping potential of unit #5 drops to almost 0% and unit #4's trapping potential becomes significant. Units #1 and #4 trapping potentials dominate for this point until the maximum suction of 1000 meters is reached.

interface #	h=0m	h=-20m	h=-40m	h=-100m	h=-1000m
1	4%	38%	59%	75%	98%
2	64%	10%	4%	0%	0%
3	1%	1%	0%	1%	5%
4	2%	1%	0%	29%	100%
5	2%	19%	42%	0%	0%

indicated that interfaces 1 and 4 were the most significant with trapping potentials of 96% and 91% respectively. While much lower, the potential for trapping at interfaces of 3 and 5 cannot be discounted. Trapping at interface 2, under these conditions seems remote.

Project terminated end of January 1996 due to CNWRA re-organization.

No more entries beyond this point

3/21/96

Pages 39 Through 149 Are Intentionally Left Blank

9-15-95
TJT

Hypothesis

Draining:

Because of the different properties of the different layers in Yucca Mountain there exist a potential for trapping to occur thus producing perched water bodies. A 1 dimensional model has already been used as a preliminary indication of the trapping potential of the area (pp. 25-37). A one dimensional simulation, though, gives a projection that is likely not very realistic so a 2 dimensional representation now being used to give a more realistic assessment of the movement of water in the area.

Initially some certain amount of water resided in the subsurface and it was assumed to be uniformly distributed throughout. This was allowed to drain on its own with no inflow. The orientation of the beds and the contrasting hydrologic properties of the various layers will cause the flow of the water to be channeled as it drains instead of just draining straight downward. This redistribution of the initial water may cause it to become more concentrated at some areas and less concentrated at others. The saturation levels at the regions of concentration may become high enough that it forms a region that is for all practical purposes a perched water body. Given enough time, all of the initial water will drain leaving the saturation levels at their irreducible minimum water content.

Flux:

The next step is to try to determine if it is possible for a perched water body

to form and be maintained from the completely drained system, (from the previous step), with a flux added uniformly at the top. If this is possible, then the smallest flux to produce this perching needs to be determined.

At some time in the past, the climate in the Yucca Mountain region was cooler and wetter than at present. This would have produced a greater overall saturation level and a higher water table than exists at present. If a particular flux could have produced a perched water body from a completely drained initial condition then it stands to reason that the same flux could produce and maintain a perched water table from a starting condition of higher overall saturation levels.

If a perching situation could be produced and maintained from a totally drained starting condition and from a relatively more saturated initial condition, (representing cooler and wetter climatic conditions of the past), then three questions are asked: 1) what is the volume of water in the perched water body produced from the drained initial condition, 2) what is the volume of water in the perched water body produced from the relatively saturated initial condition, 3) assuming the same flux and same location for both situations, how do the volumes compare. If the volumes are nearly the same (and remain so indefinitely) then it is reasonable to assert that the volume of water produced in the perched water bodies is independant of the initial saturation of the rock units involved.

Modeled area:

The region of consideration for this work is around the intersection of the

Ghostdance fault and the Sundance fault in the repository area of Yucca Mountain (figure 1). It is approximately 1100 meters X 650 meters, (width X depth). The plane of view for the simulations is the plane of the Sundance fault looking northward. The area of importance is above the water table and primarily updip from the fault. The right border of this model represents an "artificial" no-flow boundary. This causes water to accumulate here in the model whereas in actuality the flow would continue downdip here. The beds that we are dealing with are (from top to bottom : Tiva Canyon (bed 1), Paintbrush Tuff (bed 2), Topopah Spring 1,2,3 (bed 3), Calico Hills (bed 4) and Prow Pass (bed 5).

Directory and file naming convention:

All of the computer simulations were run in sebastian/ttolley/bigflo.

The code used was "BIGFLOW: A Numerical Code for Simulating Flow in Variably saturated, Heterogeneous Geologic Media", version 1.1, May 1993, by R. Ababou and A. C. Bagtzoglou, NUREG/6028, CNWRA 92-026. The individual runs of bigflo2.x. were run under directory /bigflo/run. The results of each run were placed in another directory named for the run number. For example, /bigflo/run/R01 for run #1 and no flux is indicated so this is a draining simulation. For runs where a flux was added, the word flux is added and a number indicating the amount of flux is indicated. For example, "Rflux=05." indicates that for this run 5.0 mm/year of flux was applied to the simulation. These directories contained the head levels taken at time increments in the simulation. File "HEAD_T2" indicates that the these head levels were taken at

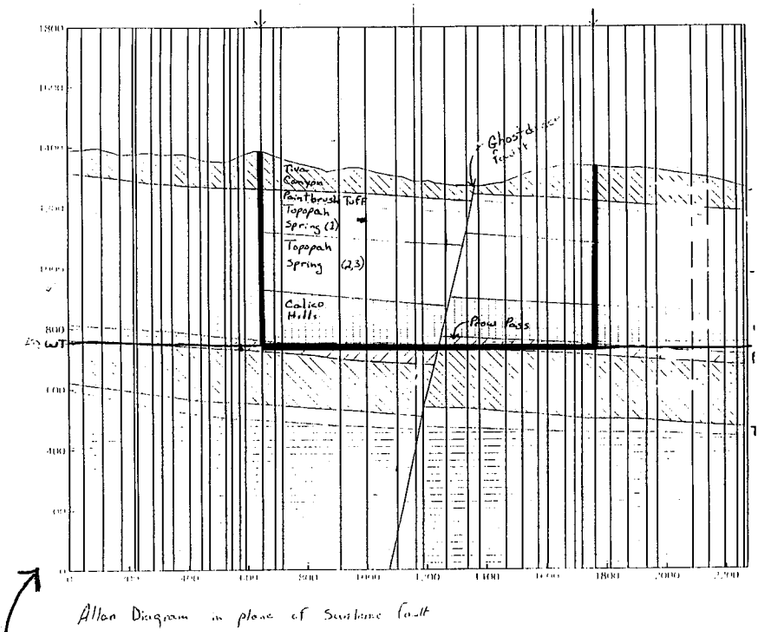

Allen Diagram in plane of Sundance fault

FIGURE 1A

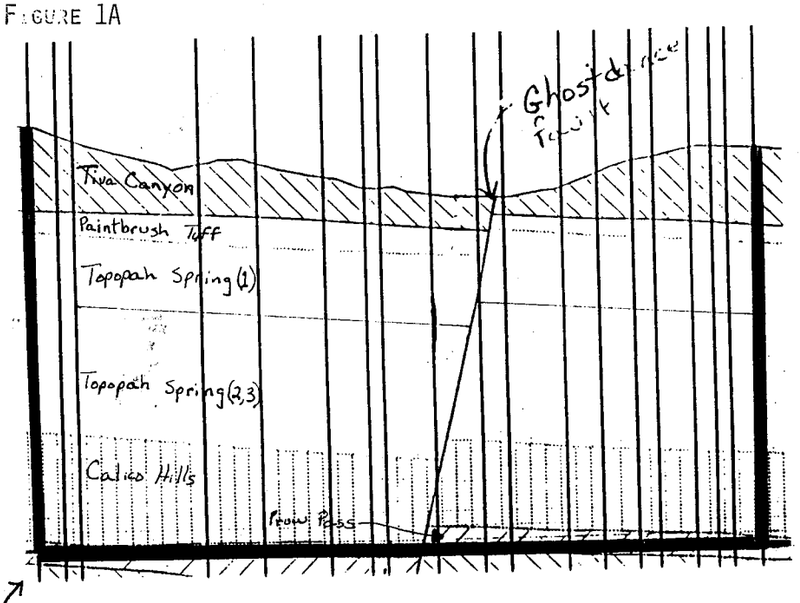

FIGURE 1B

12-18-95 TT Tolley

the second time interval in the simulation. These head values were processed for graphing in "Tecplot" in the directory /bigflo/tec. Once again individual directories were made for the individual runs using the same naming method. In these directories, (ie. /tec/R06), the head values were preplotted for "Tecplot" and the resulting Tecplot figures for head levels were stored here. In each of these directories another directory, called "flux", was created to compute the saturations, preplot the results and store the resulting graphs.

Procedures & Results 10-24-95 TTT

An initial head level was assumed to be -10 meters throughout the area of simulation and from this level a simulation of was run in in the code "figflo2.x" in increments for a cummulative time of about 158,000 years. (This was done on Sebastian/ttolley/bigflo/run/R01 ... R10, with R01 through R10 being directories for the individual increments or 'runs" of the 158,000 years). These results were further processed in sebastian/ttolley/bigflo/tec/R01.../R10 to produce an output ready to plot with "Tecplot". In Tecplot the head levels were contoured and plotted to give a visual representation of the numerical values. The head levels were initially relatively uniform. With the progression of time in the simulation, the head levels in certain areas decreased. Specifically these areas were: the updip portions of all layers, and all of bed 2 and bed 4 (except near the fault in the updip side of bed 2), (Figure 2). The interface between bed 2 and bed 3 seems to act as a barrier to vertical flow, instead channeling the water in bed 2 downdip until it encounters the fault. This point,

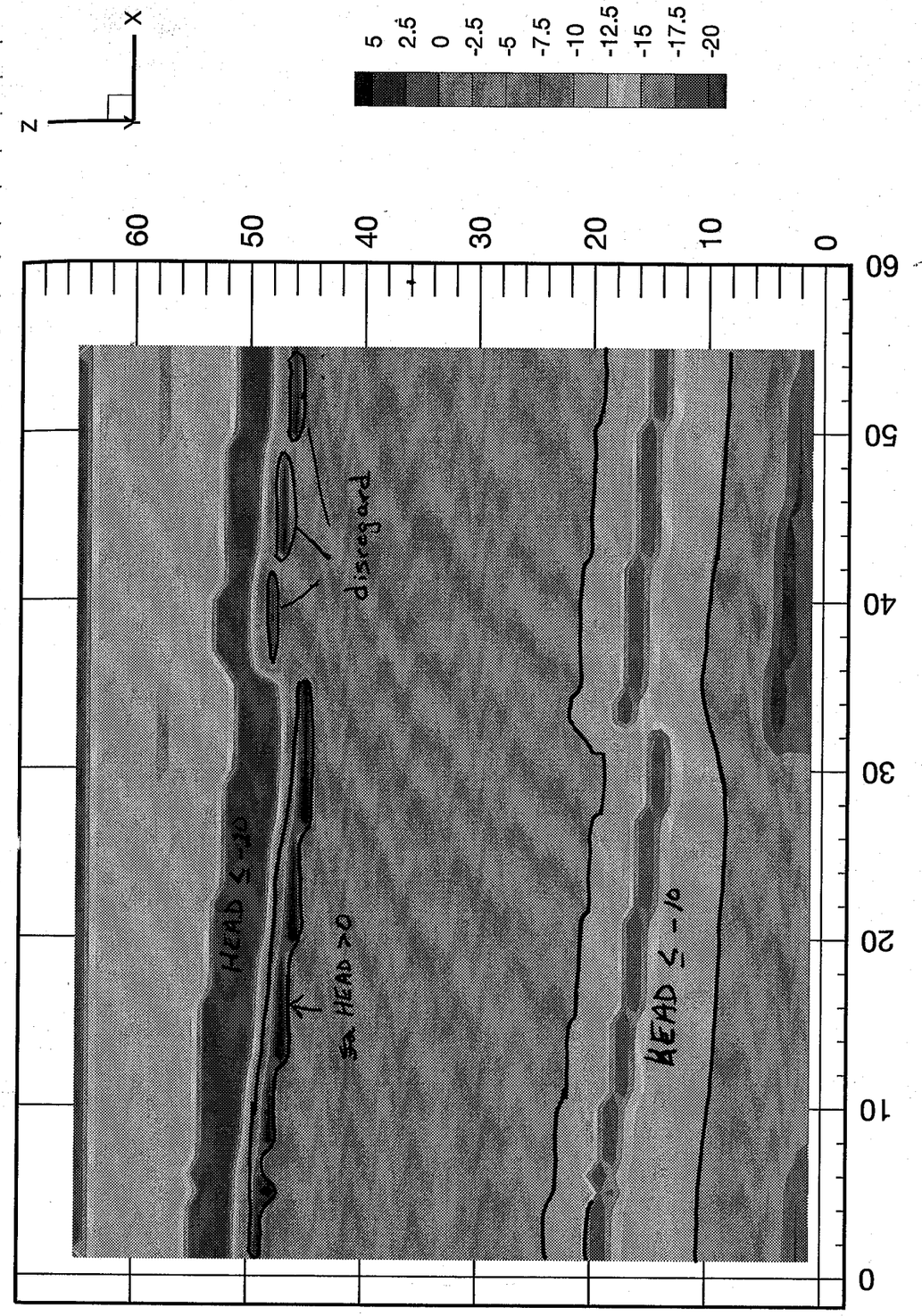

Figure 2

the intersection of bed 2, bed 3 and the fault, is the location where the higher head values begin. This region of high head values indicates higher saturation levels. Thus the water is becoming "backed up" at this point.

Although the water begins to accumulate at this point, it is, of course, not a total barrier. Rather, the water does pass across the interface from bed 2 to bed 3 but the lower hydraulic conductivity, K, of bed 3 slows the flow across the interface and instead channels it downdip until it encounters the fault. From the accumulation of water at this 3-point intersection, the flow is downward and outward. The lower K of bed 2 keeps the water from dispersing more rapidly than it accumulates thus causing a rather large region of high head values in bed 3, originating at the 3-point intersection and extending downward and outward. The fault further inhibits flow thus most of the region of high head values in bed 3 is updip from the fault.

The head values then, are initially the same throughout the simulation area. With time a region of high head values develops at the intersection of bed 2, bed 3 and the fault and extends downward and outward from this point with the main area being updip from the fault. This culminates with the maximum area of head values higher than "0" occurring at about 450 years (R07/HEAD_T03), (Figure 3). From this time onward less water is available, since the system is receiving no recharge, and the dispersion rate becomes greater than the accumulation rate. The area of head > 0 decreases and by 1600 years, (R09b/HEAD_T08), it is completely gone (Figure 4).

From each of the directories of the individual runs, (sebastian/ttolley/bigflo/tec/R01.../R10), another directory, called "flux", was created

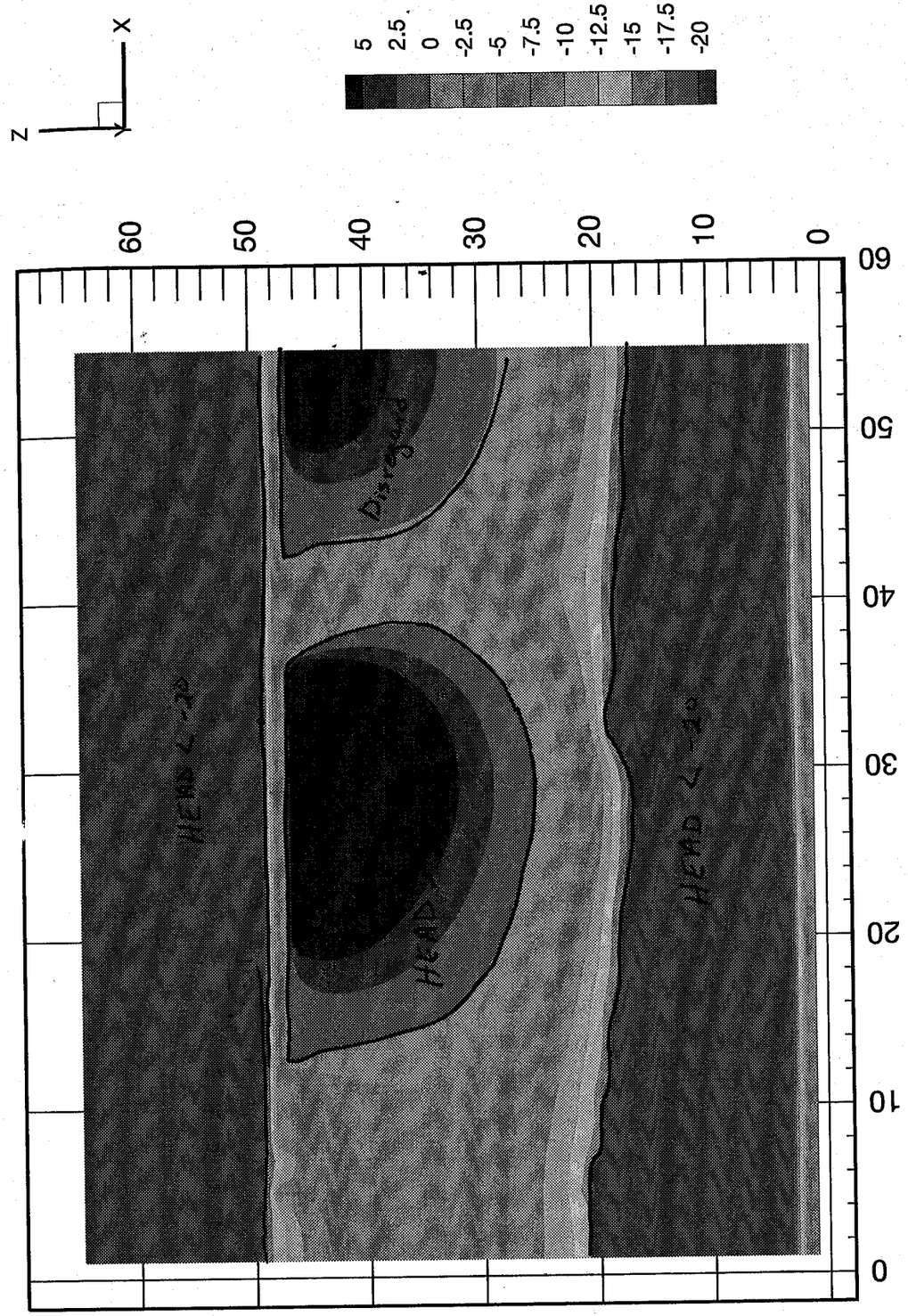

Figure 3

R07/HEADT3

T.T. Tolley 12-18-95

T L Tolley 12-18-95

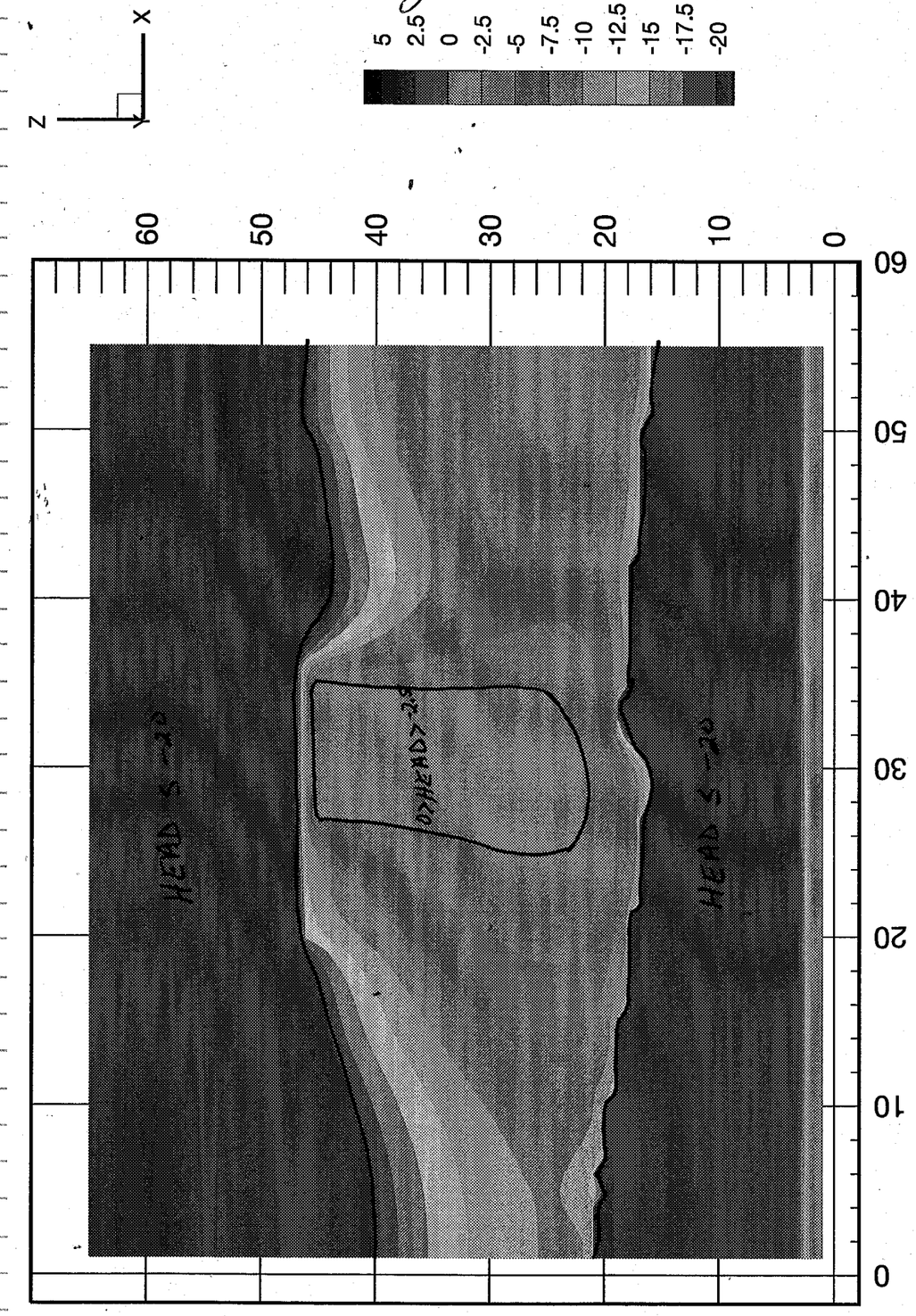

Figure 4

T L Tolley 12-18-95

to calculate the saturation levels for the corresponding head values. The head values, (output of bigflo2.x), post-processed to produce either unsaturated moisture content files, "out2_ttuns", stored as "hxx.ttuns", and saturation files stored as "hxx.sat". In all this, "xx" indicates the particular head file. These saturation levels were also plotted in "Tecplot". Only saturation levels of 99.9% or greater were considered to be fully saturated. The overall pattern for saturation levels was the same as for the head levels; regions of saturation begin to occur along the bed2/bed3/fault interface, the maximum area of saturation occurs at about 450 years, (R07h3sat), and by 1628 years, (R09b_h09sat) no saturated regions remain (Figures 5, 6, 7). The region of saturation, of course, is basically the same as the region of maximum head values.

Adding flux from completely drained

11-28-95 TLT

After determining the behavior of water in a draining simulation, (with no flux added), the question is "can a saturated zone be produced by adding flux to a completely drained system". A flux was added to the drained system in a simulation to answer this question. The system was allowed to drain for about 158,000 years with no flux, in order to assure a completely drained initial condition for the system. The head levels at the end of the draining period, R10HEAD_Txx, were now the initial head levels.The simulation was now run with the same system, except that the initial head levels were the completely drained values from R10HEAD_Txx and a flux was now added. Initially a flux of .1mm/year was added uniformly at the top. When this failed to produce a zone in which the saturation was greater than 99.9%, (essentually fully saturated), 1mm/year was

12-18-95

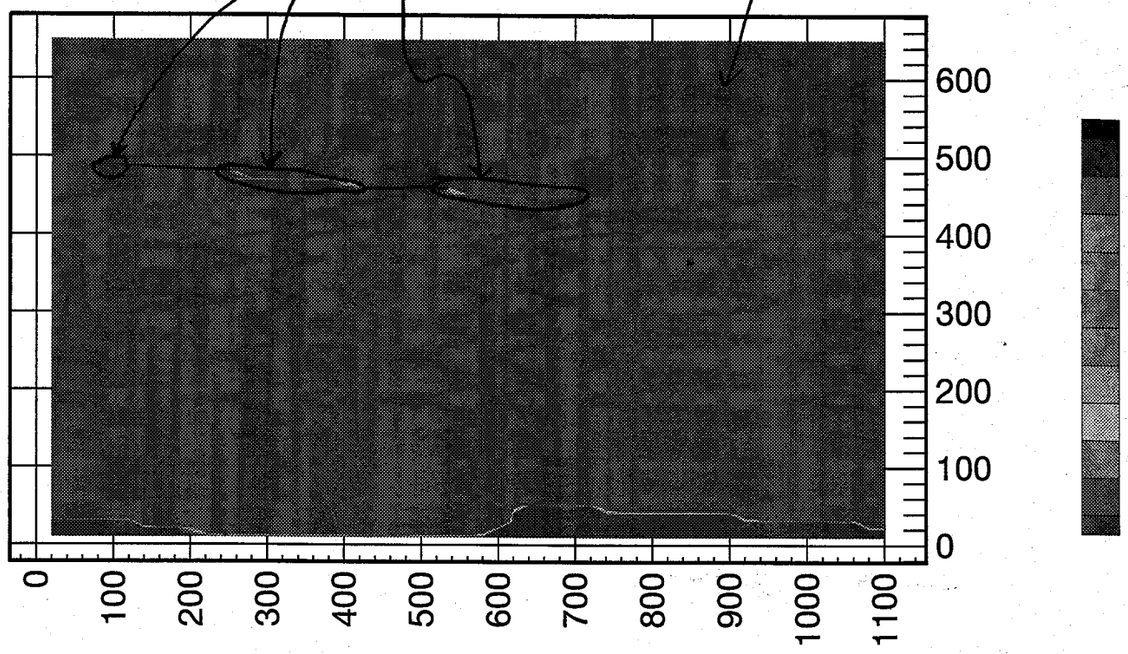

R04/h5sat
Figure 5

T J Tolly

12-18-95

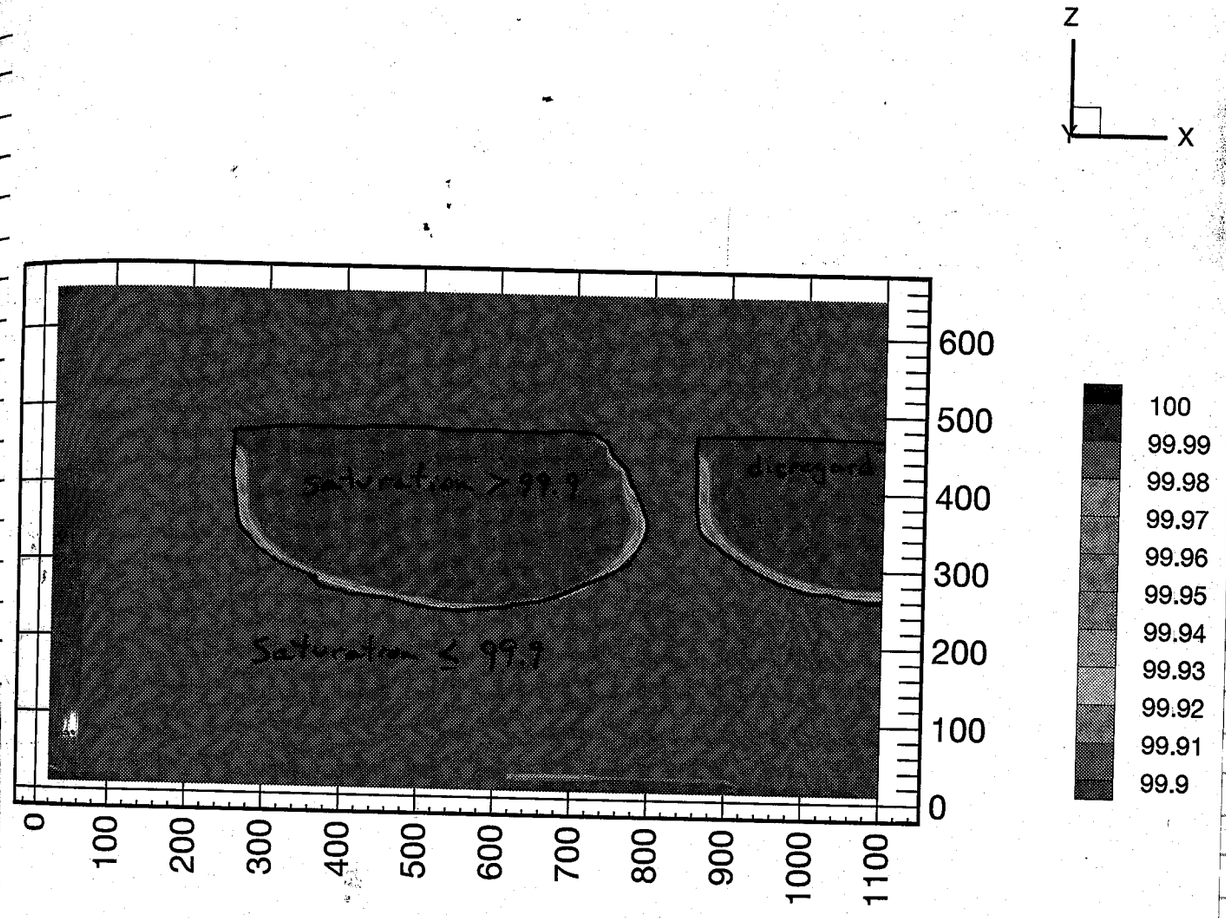

R07/h3sat
Figure 6

T J Tolly

TJTolley 12-18-95

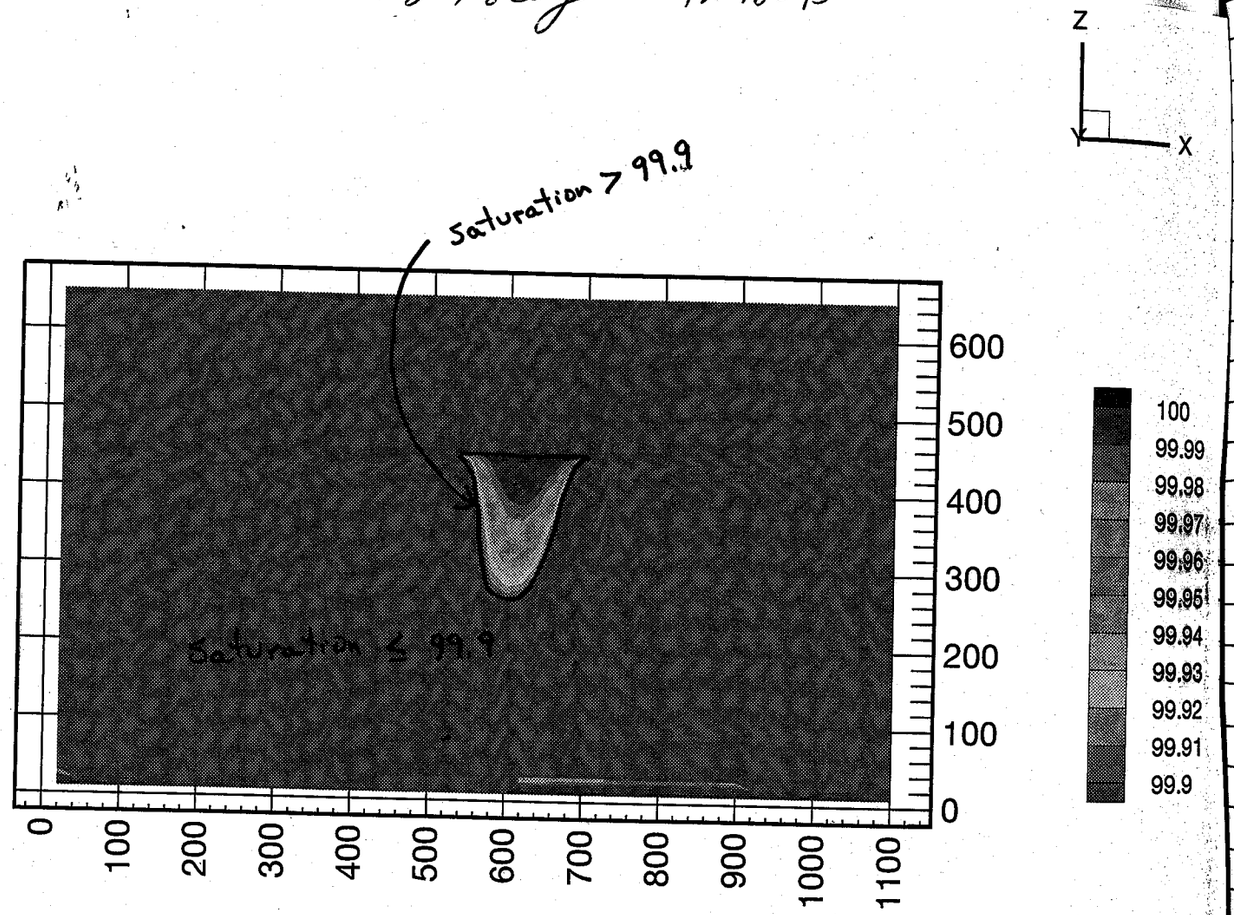

R09b/h08sat
Figure 7

TJTolley 12-18-95

added then 2mm/year, then 4mm/year was added. Finally, 8mm/year produced an perched zone, (saturation > 99.9%). Upon further evaluation it was determined that a flux of 5mm/year did not produce a perched water body but a flux of 6mm/year did produce a perched water body. The area of perching reached a maximum at about 7000 years after the flux was first added and it remained at this level for the remainder of the 19000 year simulation. While a flux of less than 5mm/year or less produced no saturated zone, one particular region, the same general region that became saturated in the draining simulation, had a progressively increasing saturation level as the flux was increased.

Thus it is possible to produce and maintain a perched water body in the region with a sustained flux.

12-6-95 TJT

Flux added to the maximum perched volume in draining simulation

Knowing that perched water bodies can be produced during the course of draining-only and from a completely drained system with a flux added uniformly to the top, it seems reasonable that adding flux to a system that already has a saturated region will sustain saturation at some level. To confirm this, another simulation was run in which the initial head levels were taken from R07HEADT3, (Figure 3), the time in the draining simulation at which the greatest area of perching occurred, (450 years). As in the case of adding flux to a completely drained system, a flux of 5mm/year did not sustain perching while with 6mm/year perching was sustained.

T J Tolley 12-18-95

12-14-95
TJT

Compare "flux added to drained system" simulation with "flux added to a saturated system" simulation

The question now is, "how do the volumes of perched water compare from these two senarios". To get a more precise value of the volumes than can be discerned from the colored contour graphs of saturation, the volume of water in each cell was computed based on its porosity and saturation and then totals the volumes of the cells that have greater than a user specified saturation level, (99.9% saturated in this case). Also in this case, 12 columns, (240 meters), on the sides, and 5 rows, (50 meters), on the bottom were ignored to eliminate "edge effects". The volumes for the simulation that added 6mm/year of flux to a drained initial condition had a final sustained volume of 5670 m^3 in the saturated zone. For the simulation that used the head values from the time of greatest perching in the draining simulation, the final sustained volume of the perched zone was 6087 m^3. The values are within about 400 m^3 of each other (or about 7%), (Figure 8). The difference is considered acceptable and is attributed to the nonlinear nature of the unsaturated flow equation.

More simulations were run with a flux between 5mm/year and 6mm/year. The initial head levels for these simulations were those of R07/HEAD_T3, (the maximum saturated condition from the draining simulation). Thus far only the volumes after about 19,000 years has been computed and only for the following fluxes: 5.0mm/year, 5.1mm/year, 5.2mm/year, 5.3mm/year, 5.5mm/year and 6mm/year.

T J Tolley 12-18-95

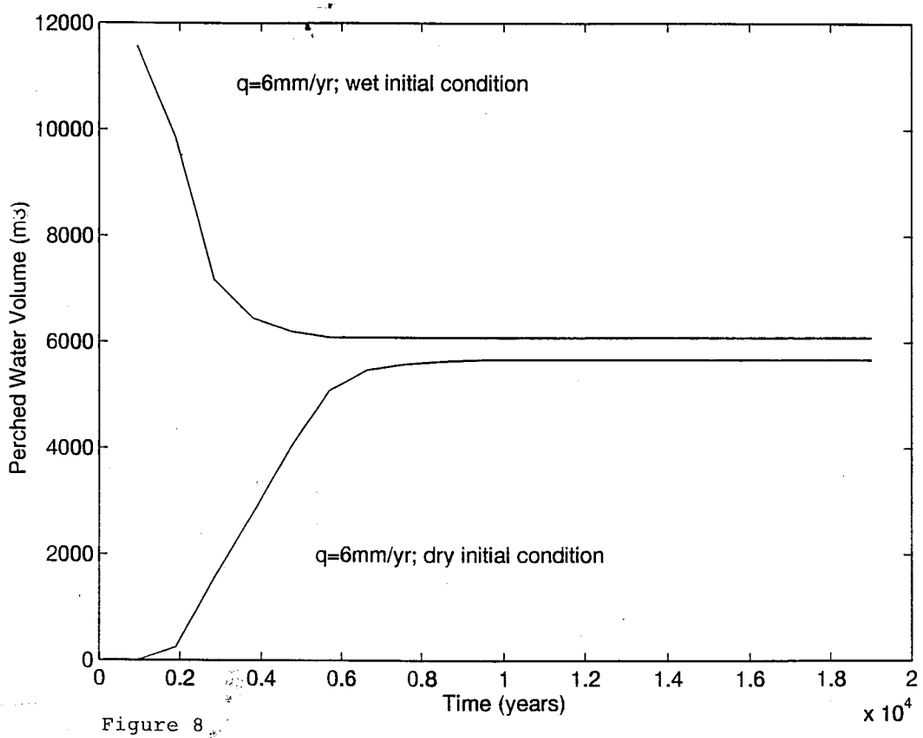

Figure 8

T J Tolley 12-18-95

The volumes for each are:

5.0mm/year	55.54 m^3
5.1mm/year	639 m^3
5.2mm/year	1195 m^3
5.3mm/year	1640 m^3
5.4mm/year	xxxx m^3
5.5mm/year	2668 m^3
6.0mm/year	6087 m^3

Thus it seems that for a given area that will allow perching to develop, the volume of perched water will be dependant upon the flux rate.

Project terminated at the end of January 1996, due to CNWRA reorganization.

No entries beyond this point

3/21/96

ADDITIONAL INFORMATION FOR SCIENTIFIC NOTEBOOK #: 148

Document Date:	05/09/1995
Availability:	Southwest Research Institute® Center for Nuclear Waste Regulatory Analyses 6220 Culebra Road San Antonio, Texas 78228
Contact:	Southwest Research Institute® Center for Nuclear Waste Regulatory Analyses 6220 Culebra Road San Antonio, Texas 78228 Attn.: Director of Administration 210.522.5054
Data Sensitivity:	■"Non-Sensitive" □ Sensitive □"Non-Sensitive - Copyright" □ Sensitive - Copyright
Date Generated:	01/13/1995
Operating System: (including version number)	NA
Application Used: (including version number)	QuatroPro
Media Type: (CDs, 3 1/2, 5 1/4 disks, etc.)	2 - 3 ½ disks
File Types: (.exe, .bat, .zip, etc.)	prn, WQl
Remarks: (computer runs, etc.)	Media contains: Mineral weight percent; isotopes data.